Senior Thesis

# Ground Penetrating Radar: Antenna Effects and Patterns.

By
Jess Bookshar
1998

Submitted as partial fulfillment of
the requirements for the degree of
Bachelor of Science in Geological
Sciences at The Ohio State University
Spring Quarter 1998

Approved by:

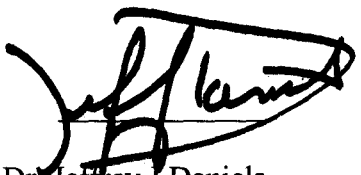

Dr. Jeffrey J Daniels

Table of Contents

## List Of Figures and Appendices

## Abstract

In the spring of 1998, 816 lines of Ground Penetrating Radar (GPR) data were recorded to determine the effects of antenna orientation on reflection data. The large amount of data collected allowed for the investigation of many variables that affect GPR data. One of the few variables that can actually be changed in field situations, (in other words not inherent to the target) is antenna orientation. The importance of different antenna orientations is demonstrated within. After the data was processed and put into visual form, comparisons could be made, and conclusions and generalizations were possible based upon them. The requirements for the detection of a target include the following: 1) a sufficiently strong input wave is needed, 2) the impedance contrast needs to be high enough for a reflection, 3) the target size needs to be sufficient for the burial depth, and 4) other objects must not interfere. The effects of target size, target type, burial depth, offset, and antenna orientation are shown. Polarization, and therefore antenna orientation, is shown to have a large affect on the resulting data quality. In most situations best results were obtained with the antennas oriented perpendicular to the traverse of the line.


## Introduction

This study was undertaken, with the guidance of Dr. Daniels, in order to study the effects of different antenna variables on GPR data. A massive amount of data was collected; thirty-four lines were run for two target types (conductor and dielectric), of three sizes (2", 6", and 11" diameters), at two burial depths (1' and 2'), and with two antenna orientations (parallel and

perpendicular to traverse), for a total of 816 traverse lines of data. This provided ample data for the study of a number of factors. Target shape and orientation were not among these, because perfect spheres were used. However, by using a perfect sphere, the effects of polarization could also be studied. A uniform sphere gives the same reflection, for the same incident energy, in any direction. Any variations with respect to antenna orientation and offset, other than a steady increase in two way travel time with offset, must be due to polarization.

## Section 1: GPR concepts

Ground Penetrating Radar is a relatively new shallow subsurface exploration tool, dating back no further than approximately 1970. It is based on the response of electromagnetic radiation to boundaries in the subsurface. The radiation does one or more of three things at a boundary; it is reflected, refracted, or diffracted. These boundaries are defined by an electrical properties (or impedance) contrast, which arises from conductivity, and permittivity variations. These contrasts show up in GPR records as anomalies. It is the identification, interpretation, and manipulation of these anomalies that is the key to determining the existence, depth and physical characteristics of a buried target.

The source for the electromagnetic radiation is a transmitting antenna. A commercially available GSSI 500 MHz antenna (with a SIR-10 control unit) was used for these experiments, but there is a wide range of antenna types, with each one designed for specific ground conditions. GPR antennas are generally wide band, and are identified by their center band frequency. A higher frequency antenna allows for greater resolution, and less penetration, while a lower frequency will go further into the earth at the cost of resolution. The properties of the ground can

not be changed, but the antenna characteristics can be manipulated to improve records. The antenna sends a pulse of radiation into the ground. However, before it even reaches the host rock, the signal is subject to interference from system electronics, internal coupling, and the electrical properties of the air-ground interface.

The electromagnetic wave propagates through the host material until it reaches an impedance contrast, at which point it is reflected (figure 1). An impedance contrast is a difference in electrical properties that causes electromagnetic energy to scatter. The strength of this reflection is proportional to the contrast in impedance. The reflected wave can travel back through the medium and be detected by a receiving antenna. The transmitting and receiving antennas can be separate (bistatic) or one antenna can be used for both transmitting and receiving (monostatic). The orientation of the antennas can be of great importance, as will be discussed later.

The reflections are recorded digitally over a certain time interval, which depends on the speed of the wave through the medium, or propagation velocity. A two way travel time is what is measured, where: $t_d=2Z/V$

$t_d$ is the two way travel time in nanoseconds

Z is depth to target in meters

V is propagation velocity in meters per second

The dominant factor allowing for propagation is the relative electric permittivity. A low relative permittivity yields a high velocity, and a high relative permittivity yields a lower velocity.

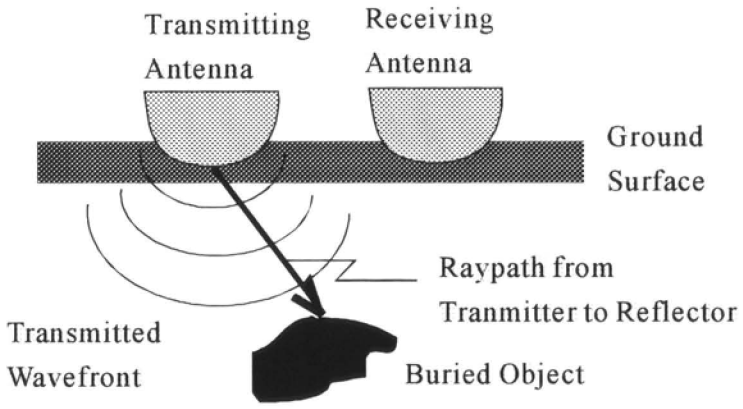


(a) Radar wave transmitted as a cylindric spreading wave.

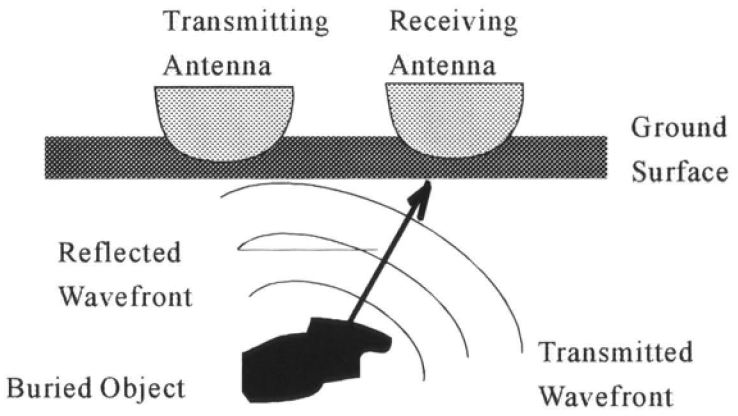


(b) Reflected wave from a point on a buried object.

Figure 1. The GPR reflection process. The wavefront spreads out from the transmitting antenna and reflects from the buried object, before it is detected by the recieving antenna. (From Daniels, 1994)

One set of a transmitted and received signal, with reflection if present, is called a trace. By assigning a shade of gray to amplitude ranges and placing successive traces of a line side by side, a gray-scale cross section is generated. This process is illustrated in figures 2 and 3. Displaying successive lines side by side yields a three dimensional time image of the subsurface as shown in figure 4. Noise and clutter are also present on the records, and all GPR data needs to be interpreted to separate reflections from noise. Noise and clutter can either mask a reflection, or appear to be something that is not there. Noise is a signal from outside phenomena (like radio interference), clutter is reflected energy from targets other than the target of interest. Filtering and stacking of data can often overcome this.

In order for the system to detect an object, the following conditions must be met: 1) the transmitted wave must be strong enough to go to the buried object and return to the surface, 2) the impedance contrast must be high enough, 3) the object must be large enough to be detected at that depth, and 4) Other objects must not interfere.

## Section 2:Fundamentals of Polarization

Propagation and polarization control how and if electromagnetic radiation gets from the source, into the host material, to the target, and back to the receiver. Not only does the energy have to return to the receiver, but it must do so in the right orientation. If not, the reflection may appear exceptionally weak, or may not show up at all. This is where polarization becomes important. Polarization is the alignment of electromagnetic vibrations, or waves, in preferential directions. Radiation can be linear or elliptically polarized. If a unit vector is assigned to the electric field generated by the radiation, then the path that this vector follows as the wave propagates defines the polarization orientation. If it stays in one plane it is said to be plane

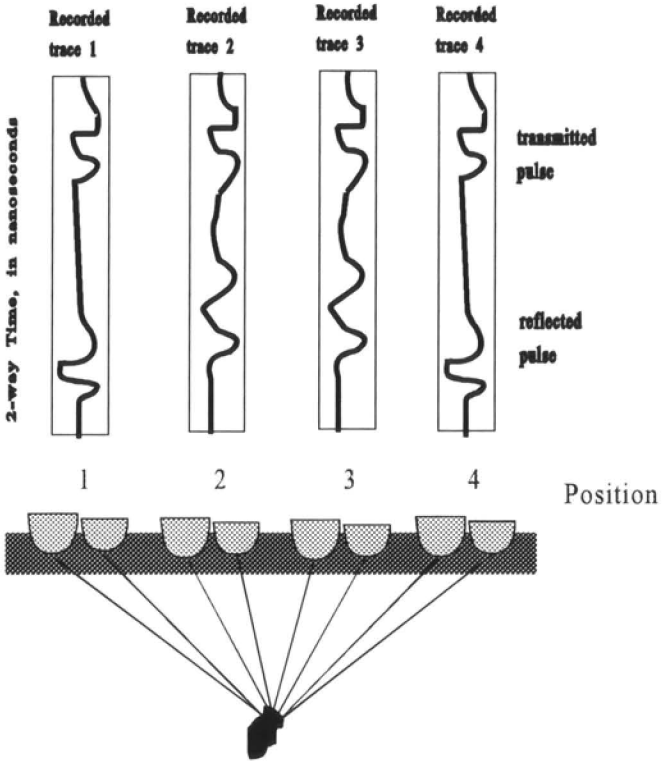


(a) Single traces recorded at different antenna locations.

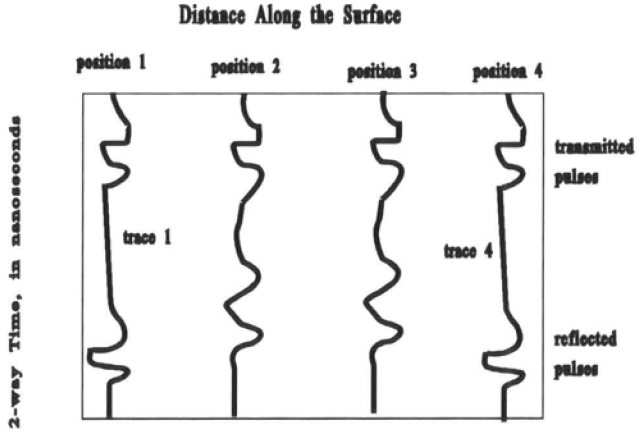


(b) Resulting 4 trace GPR record, or cross section.

**Figure 2. The process of combining traces, recorded at even spacings on the surface, to form a GPR record. (From Daniels, 1994)**

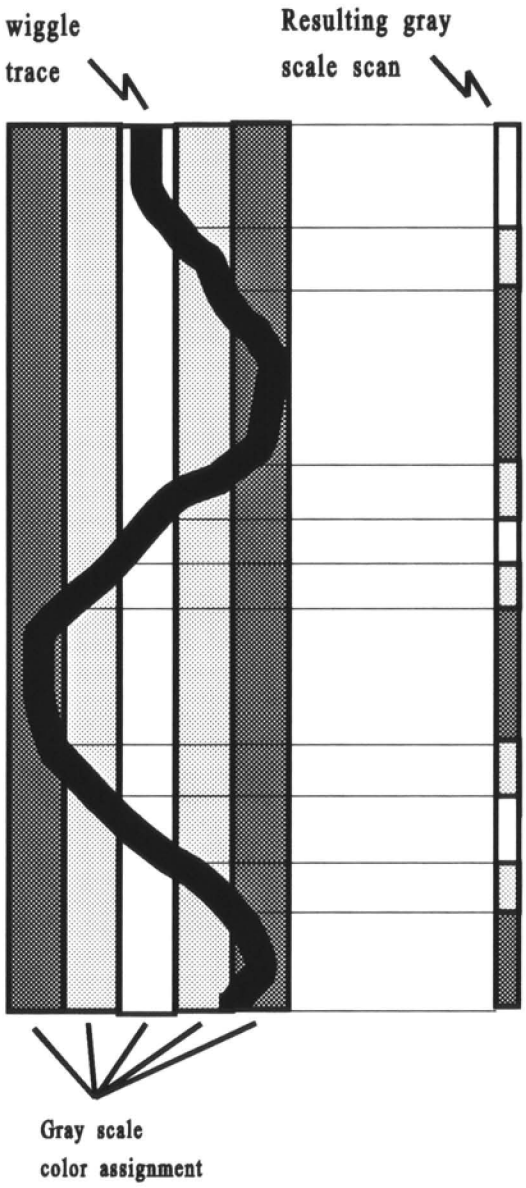


Figure 3. Gray scale (or color) assignment procedures. Gray shades are assigned to different amplitudes on the wiggle trace, producing a gray scale scan. (From Daniels, 1994)

a) 3D GPR data visulization approaches

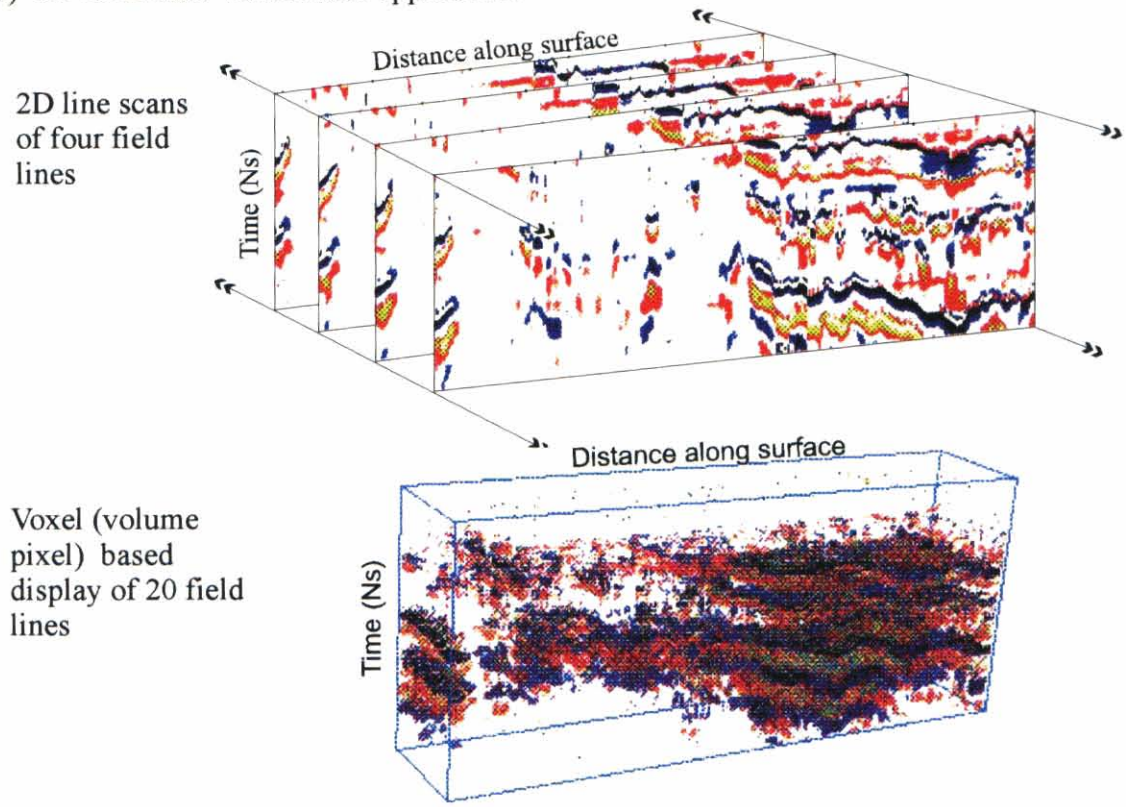


b) Different ways to slice volume data

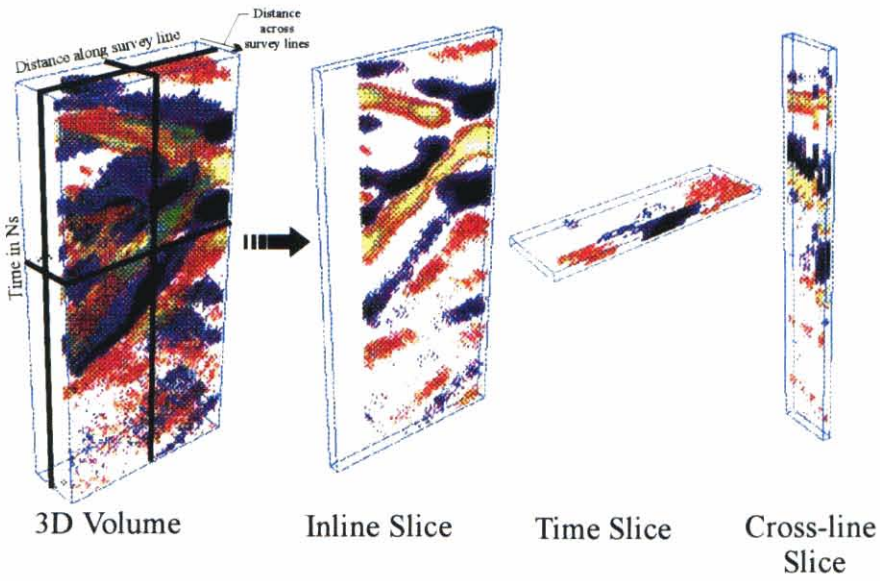


Figure 4. Different 3D volume visualization approaches using GPR data. a) comparison of data visualization using 2D line scan sections versus the voxel based approach with alpha rendering. b) Use of different types of slices of 3D GPR data to help interpretation. (From Daniels et. al. 1997)

polarized, and if it rotates around an axis parallel to the propagation direction it is elliptically polarized (Roberts, 1994). The propagating GPR wave is assumed to be planar, and GPR antennas transmit a linearly polarized field.

There are three facts important to GPR polarization phenomenon: 1) dipole transmit antennas radiate linearly polarized waves, 2) reflections or diffractions from buried targets are often depolarized (this depolarization depends upon the angle of incidence, the impedance contrast, the antenna separation, and the shape and orientation of the target, though the later are not a factor when using a uniform sphere), and 3: dipole receiver antennas are sensitive to the polarization of both reflected and refracted linearly polarized waves (modified from Roberts, 1994)

## Section 3: Methods

Measurements were carried out in a large (95"x75"x48"deep) sand box. The sand was moistened before the first set of measurements and the smoothed surface was kept covered with plastic thereafter. Three styrofoam spheres of different sizes (diameters of 2", 6", and 11") were used as targets, uncovered as dielectrics, and wrapped in aluminum foil as conductors. A particular ball size and type was buried, and measurements were carried out with two perpendicular antenna orientations. A GSSI SIR 10 system was used. A wheel was used between the SIR 10 and the bistatic (separate transmitter and receiver) antenna to trigger data sampling from the receiving antenna. The slightest turn of the wheel caused the antenna to send and receive a signal corresponding to one trace, which gave an even distribution of traces along a traverse line. An average of 273 traces per pull was recorded, and data was standardized to this. The data were named and saved on hard disk (see appendix A), on a trace-by-trace basis, with

one traverse line per stored digital file. On one side of the spherical target one line per inch spacing was used in order to achieve good resolution, while the other side was only sampled at a two inch interval between lines because of the symmetry involved. For each set of measurements 34 lines were recorded. The antenna was then realigned, perpendicular to the previous alignment, and the 34 lines were run again. Then the ball was dug out and replaced with another, with meticulous care taken to insure that the target's center did not vary between measurements at the same burial depth. The measurement process was then repeated. Collection of the entire data set was completed over a three week period during February and March of 1998.

Data manipulation was done using a program called RADACAL (developed here at Ohio State by Roger Roberts) and 3-D displays were achieved with a program called BOB. The raw data was byte-swapped, then standardized to 273 traces per line. A one-dimensional filter was then applied to the data, which basically smoothed the traces and removed the DC component of the signal. Two-dimensional images were generated with RADACAL, using a gray scale format. RADACAL essentially lined up traces, and assigned a certain part of the gray scale to each amplitude. See figures 2 and 3. Bright spots and dark spots therefore correspond to high positive or negative amplitudes, which come from the reflectors (or the input wave). The three-dimensional images were generated with BOB. Precise manipulation of the color palette with respect to amplitude was necessary to generate interpretable results. Only one polarity was used for the 3-dimensional images.

## Section 4: Results

Effect of ball size:

As was expected, the larger the sphere, the better it showed up on the records (figure 5 and Appendix B). Also, resolution with respect to offset was greater with a larger sphere. There seems to be a limit to the size of a detectable object that depends on the distance to the antenna, and the electrical properties contrast between it and the host medium for a particular frequency of the transmitted signal. This supports numbers 2 and 3 of the aforementioned requirements for detecting a buried object.

Effect of burial depth:

When a wave of electromagnetic radiation is sent into a dielectric half space (moist sand for example) the wavefront begins its traverse closely approximating a hemisphere. It reaches a point, however, at which it is more closely approximated by a plane of radiation. This distinguishes between near field and far field conditions. In the near field modeling of the wave is difficult because of signal interactions with the surface, but the far field is modeled by a plane wave. The two fields reflect data back to the receiver differently. It was hoped that some sign of this would show up on the data, but it does not appear so, though it is believed that the boundary between near and far field was somewhere between one and a half and two feet below the surface.

All the conducting spheres were easy to recognize at both burial depths. They all formed nice parabolic shaped spatial anomaly patterns, although the shapes varied somewhat with ball size (figures 6a, b and c, and Appendix B). The spheres buried at a depth of one foot have the

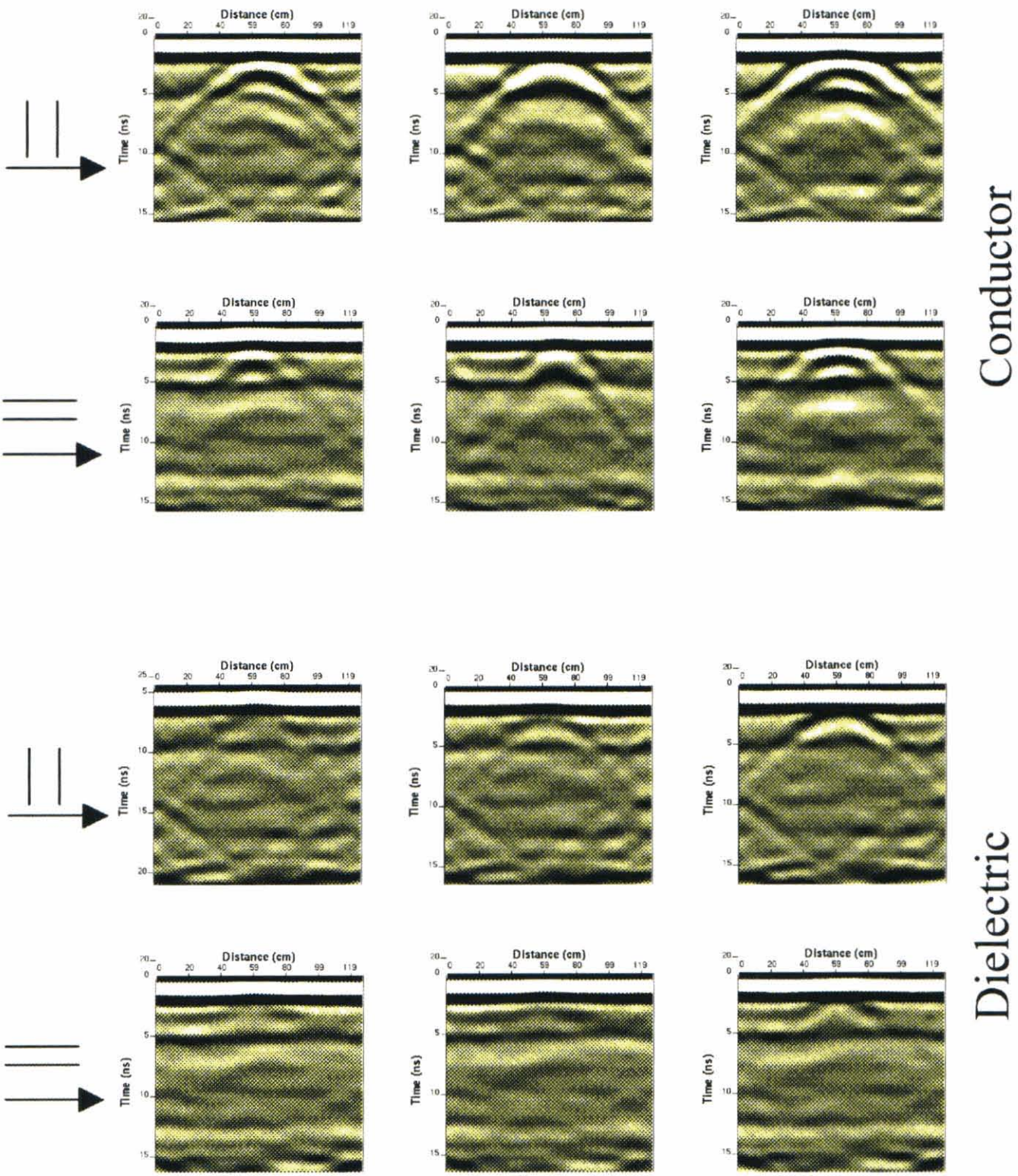


Figure 5a

Effect of ball size. Burial depth of 1 foot.
0 offset, for conductors and dielectrics.
With both antenna orientations.

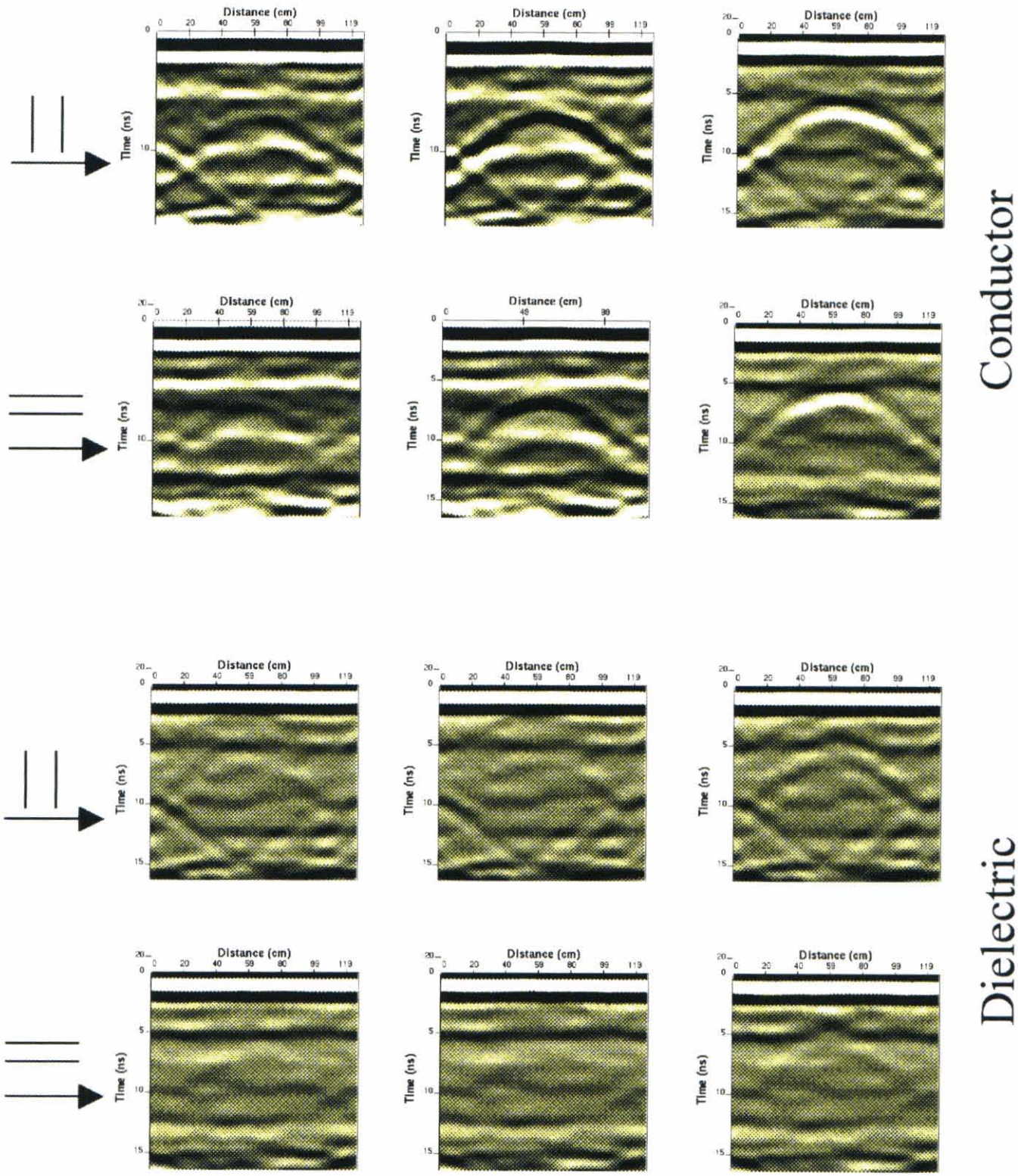


Figure 5b

Effect of ball size. Burial depth of 2 feet.
0 offset, for conductors and dielectrics.
With both antenna orientations.

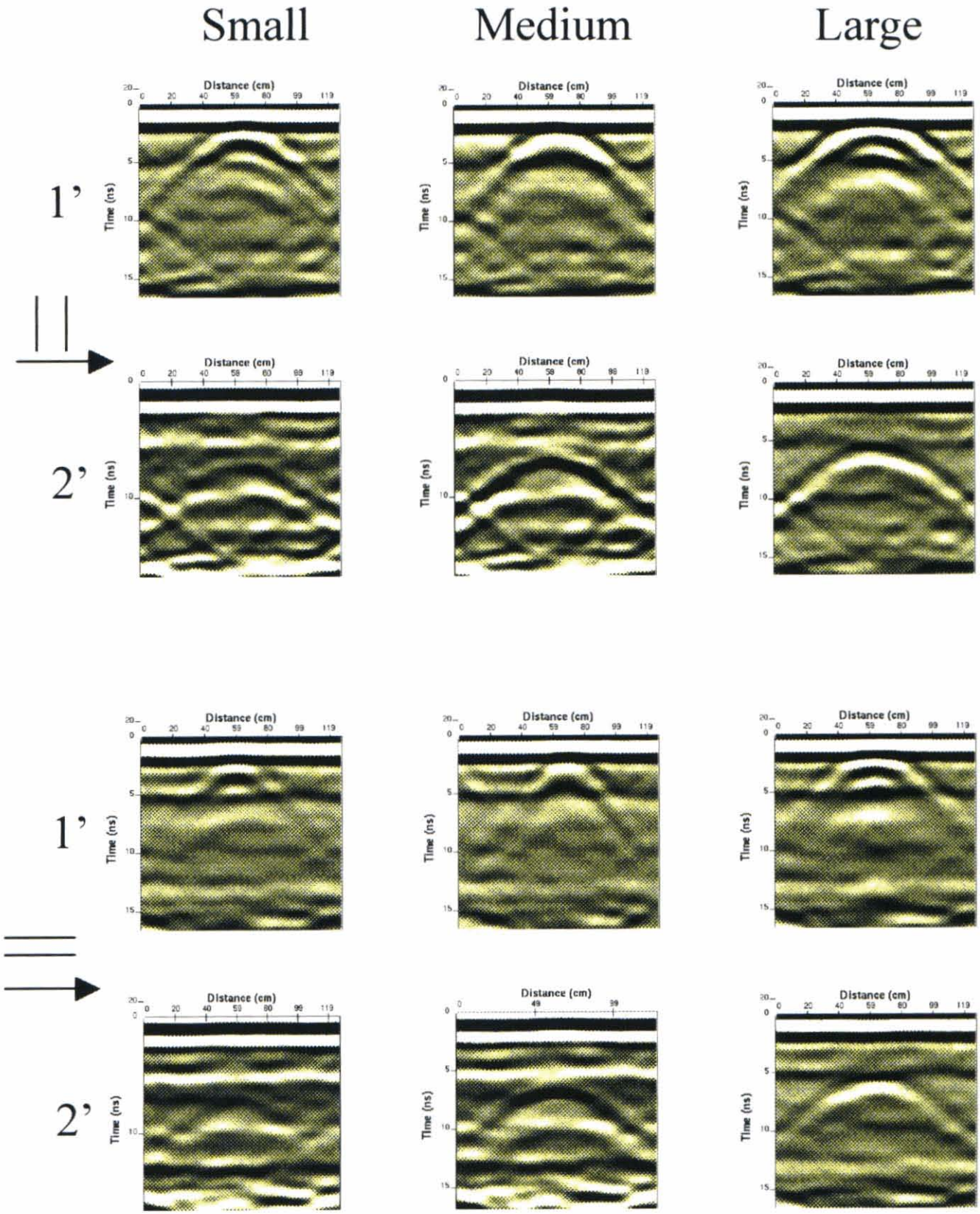


Figure 6a

Effect of burial depth. Conductors with 0 offset. Shows both antenna orientations, and all three Ball sizes.

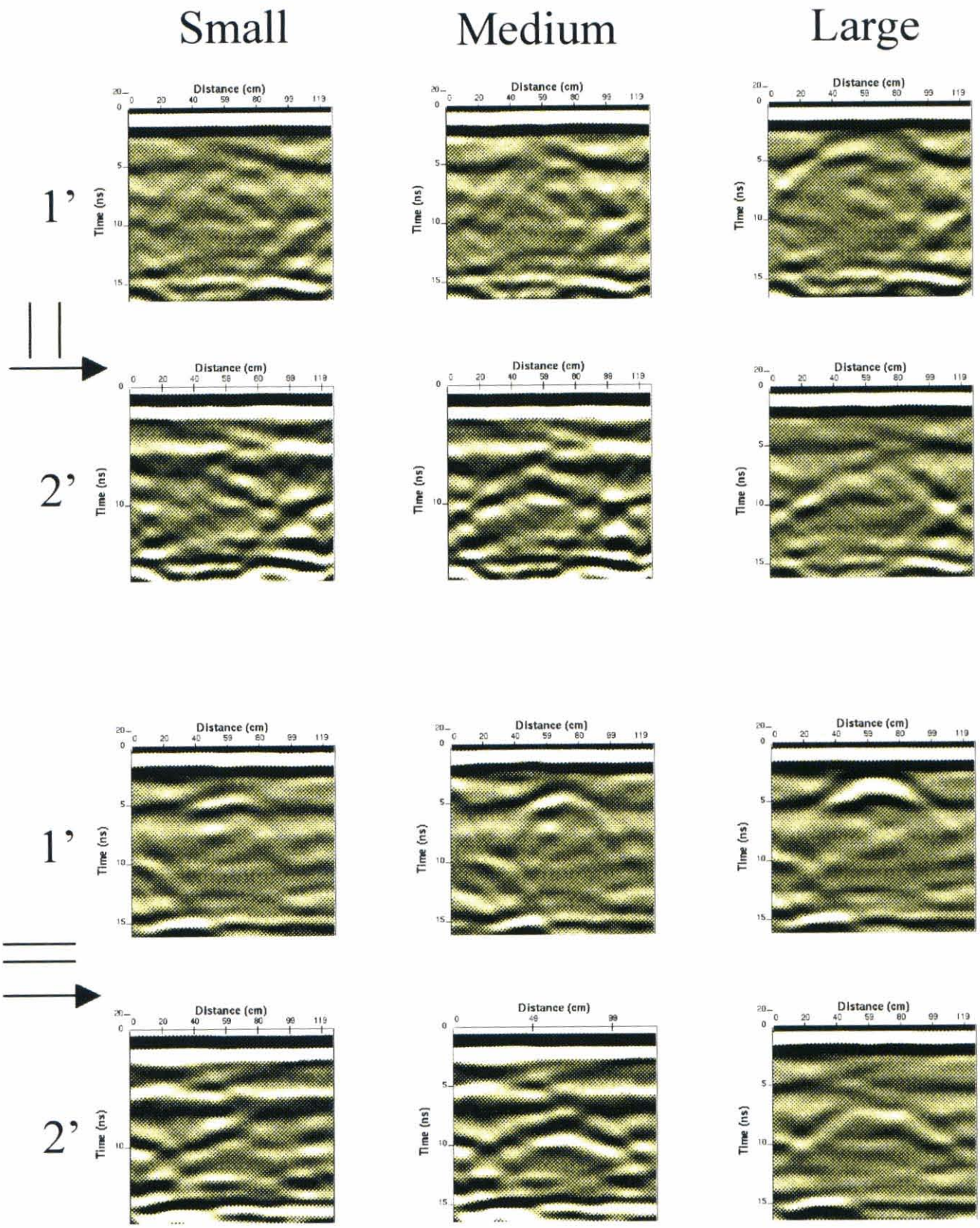


Figure 6b Effect of burial depth. Conductors with 12 inch offset. Shows both antenna orientations, and all three Ball sizes.

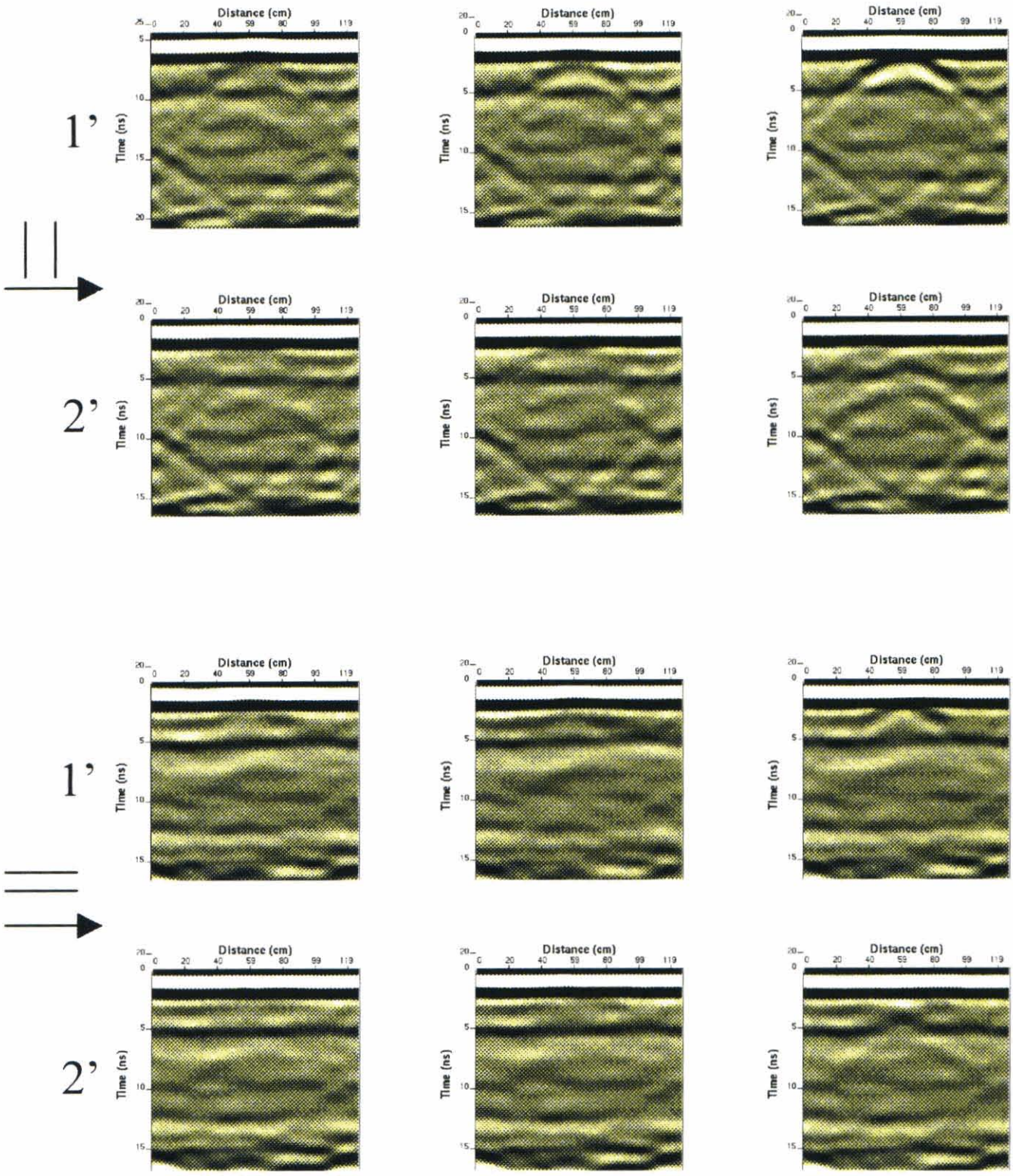


Figure 6c

Effect of burial depth. Dielectrics with 0 inch offset. Shows both antenna orientations, and all three Ball sizes.

tops of their reflections masked. This is actually the input signal interfering with the data. This anomaly is present in all of the data as two distinct bands corresponding to high amplitude positive and negative polarities associated with the input wavelet. If something uniform and continuous shows up on GPR data, then it is a good bet that it is not part of the subsurface, but rather some form of outside interference. The dielectric spheres show up at the one foot burial depth, but the small and medium dielectric spheres become hard to recognize at the two foot burial depth. Because such shallow burial depths were used, the input signal has ample strength to reach the targets and propagate back to the antenna. In fact, though masked from a lot of the images, the bottom of the pit shows up quite well on all the data. This satisfies the first requirement for target detection from above.

Effect of ball type:

The aluminum foil covered spheres used were perfect conductors, and the uncovered Styrofoam spheres were a close approximate to perfect dielectrics. Both yielded interpretable results (figure 5 and Appendix B). All the conductors show up well. Some of the records for the deeper dielectrics show little or nothing. Further filtering of the data may have been able to extract clearer images here. The reason the conductors show up so much better than the dielectrics, lies within the size of the electrical properties contrast. At the sand-conductor boundary, which sends back a strong reflection, the contrast in electrical properties is large, while at the sand-dielectric boundary the contrast is not nearly as large, hence the weaker reflection.

Effect of Offset:

Variations in amplitude caused by polarization effects and the antenna pattern were expected in the lines as offset changed, and nulls were expected on some of the lines. The nulls do in fact show up, though more frequently with the antennas oriented parallel to the direction of traverse. The two-way travel time increases as offset is increased, and the positions of the reflectors are moved to a later time on the record (figure 7, and Appendix B). Most of the spheres did not appear on the records all the way out to the maximum offset of 20 inches, and as the lines approach the 20 inch offset, the side of the pit starts to show up on the records.

Effect of Antenna Orientation:

In general, higher amplitude anomalies were achieved with the antennas oriented perpendicular to the direction of traverse than with them parallel. The parabolas are more continuous with this orientation. Nulls were recorded more often on either side of the strong central part of the record with the antennas oriented parallel to the direction of traverse (2cm and 2cmx in Appendix B). Both orientations seem to give results out to the same offset. It is important to note the large differences between the records having identical parameters, but measured with the two different orientations (Appendix B). These differences are due to polarization, and possibly depolarization, at subsurface boundaries. The antenna radiates a plane polarized wave, and the amount of energy that reaches the reflector and is reflected back from the target, and what is actually detected by the receiver depends on the orientation of the antennas with respect to the position of the target.

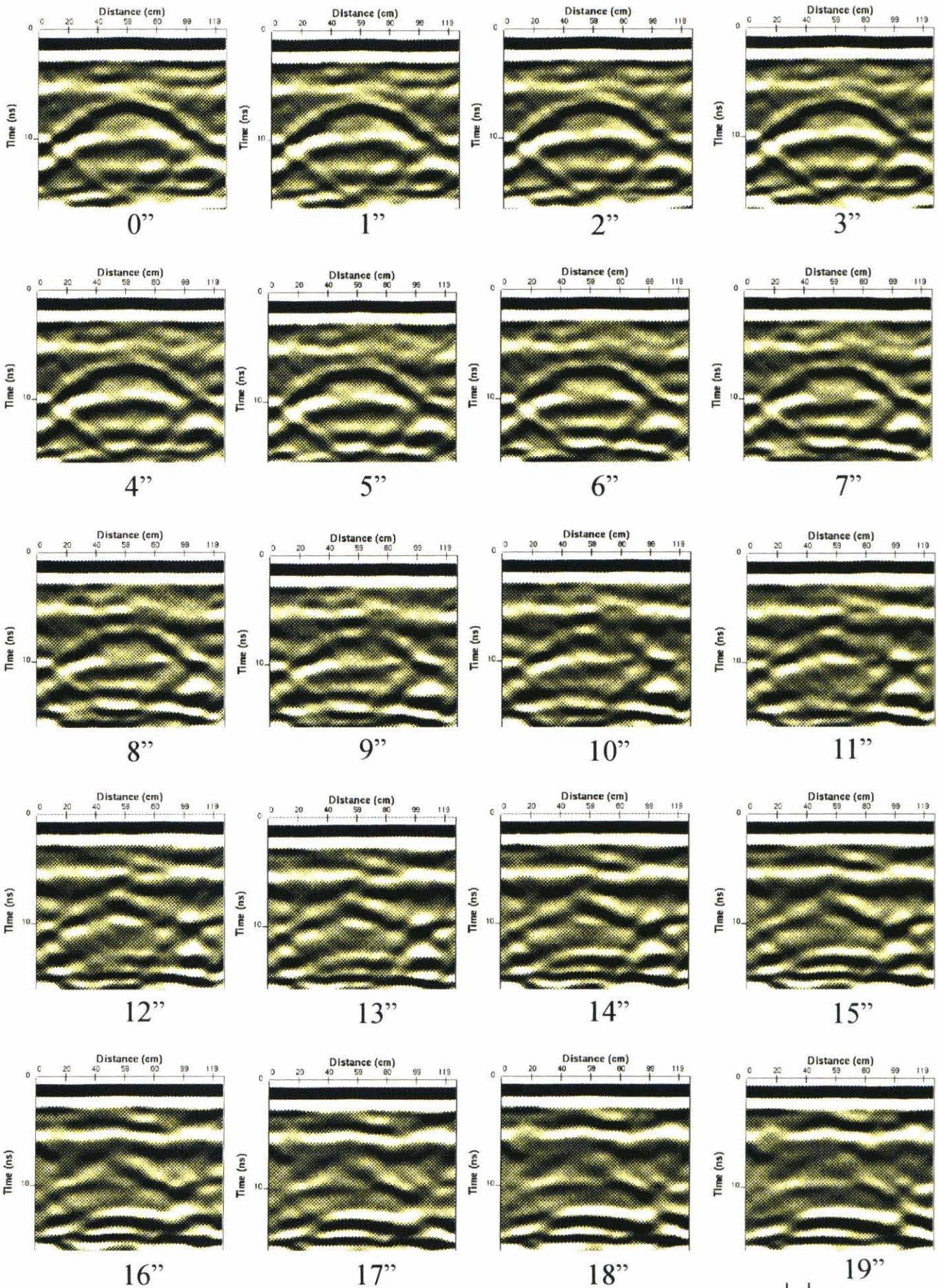


Figure 7a Effect of offset. Medium conductor buried at 2 feet.

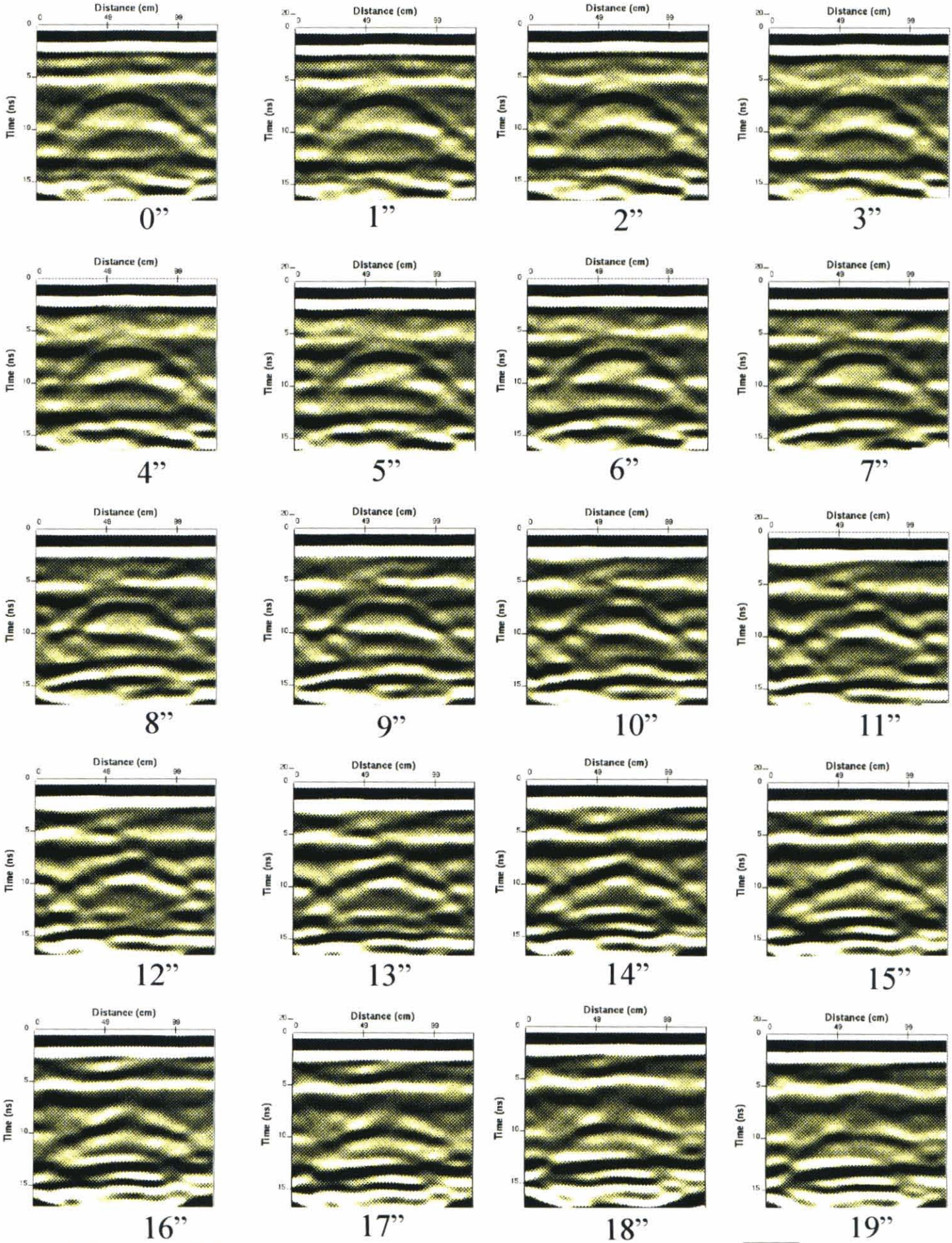


Figure 7b Effect of offset. Medium conductor buried at 2 feet

## 3-D Results

Converting the data into interpretable 3-D images required a lot of manipulation. Precise assignment of colors to amplitude ranges was key. Because the 3-D images need to be "transparent", noise and clutter on several different lines can combine to obscure the target. Further filtering of the data may have aided in the clarity of the 3-D images. Even when the 2-D data was easily interpretable, 3-D images were not always clear. As you can see in the first figure of Appendix C, when the lines are combined properly, a 3-D image can be useful. It can provide more information on the overall size of the target. The nulls caused by effects of polarization that were mentioned earlier can be seen clearly on some of the 3-D images.

## Conclusion:

One often thinks of a wave propagating through the subsurface as a uniform hemisphere, and would therefore conclude that the orientation of GPR antennas would make little difference in the resulting data. This is not the case. Because of polarization effects, and the resulting reflected wave pattern, antenna orientation becomes a key factor in identifying and interpreting anomalies associated with subsurface targets in GPR data. The data from this experiment also demonstrates, and follows the requirements for detection of a target, including: 1) the transmitted wave must be strong enough to go to the buried object and return to the surface, 2) the impedance contrast must be high enough, 3) the object must be large enough to be detected at that depth, and 4) Other objects must not interfere.

Line Names

| Distance From Center of Antenna to Center of Sphere | small conductor at 1 foot | small conductor at 1 foot w/ ant. // | small dialectric at 1 foot | small dialectric at 1 foot w/ ant. // | medium conductor at 1 foot | medium conductor at 1 foot w/ ant. // | medium dialectric at 1 foot | medium dialectric at 1 foot w/ ant. // | large conductor at 1 foot | large conductor at 1 foot w/ ant. // | large dialectric at 1 foot | large dialectric at 1 foot w/ ant. // |
|---|---|---|---|---|---|---|---|---|---|---|---|---|
| -20 | 1cs70 | 1csx70 | 1ds70 | 1dsx70 | 1cm70 | 1cmx70 | 1dm70 | 1dmx70 | 1cl70 | 1clx70 | 1dl70 | 1dlx70 |
| -18 | 1cs68 | 1csx68 | 1ds68 | 1dsx68 | 1cm68 | 1cmx68 | 1dm68 | 1dmx68 | 1cl68 | 1clx68 | 1dl68 | 1dlx68 |
| -16 | 1cs66 | 1csx66 | 1ds66 | 1dsx66 | 1cm66 | 1cmx66 | 1dm66 | 1dmx66 | 1cl66 | 1clx66 | 1dl66 | 1dlx66 |
| -14 | 1cs64 | 1csx64 | 1ds64 | 1dsx64 | 1cm64 | 1cmx64 | 1dm64 | 1dmx64 | 1cl64 | 1clx64 | 1dl64 | 1dlx64 |
| -12 | 1cs62 | 1csx62 | 1ds62 | 1dsx62 | 1cm62 | 1cmx62 | 1dm62 | 1dmx62 | 1cl62 | 1clx62 | 1dl62 | 1dlx62 |
| -10 | 1cs60 | 1csx60 | 1ds60 | 1dsx60 | 1cm60 | 1cmx60 | 1dm60 | 1dmx60 | 1cl60 | 1clx60 | 1dl60 | 1dlx60 |
| -8 | 1cs58 | 1csx58 | 1ds58 | 1dsx58 | 1cm58 | 1cmx58 | 1dm58 | 1dmx58 | 1cl58 | 1clx58 | 1dl58 | 1dlx58 |
| -6 | 1cs56 | 1csx56 | 1ds56 | 1dsx56 | 1cm56 | 1cmx56 | 1dm56 | 1dmx56 | 1cl56 | 1clx56 | 1dl56 | 1dlx56 |
| -5 | 1cs55 | 1csx55 | 1ds55 | 1dsx55 | 1cm55 | 1cmx55 | 1dm55 | 1dmx55 | 1cl55 | 1clx55 | 1dl55 | 1dlx55 |
| -4 | 1cs54 | 1csx54 | 1ds54 | 1dsx54 | 1cm54 | 1cmx54 | 1dm54 | 1dmx54 | 1cl54 | 1clx54 | 1dl54 | 1dlx54 |
| -3 | 1cs53 | 1csx53 | 1ds53 | 1dsx53 | 1cm53 | 1cmx53 | 1dm53 | 1dmx53 | 1cl53 | 1clx53 | 1dl53 | 1dlx53 |
| -2 | 1cs52 | 1csx52 | 1ds52 | 1dsx52 | 1cm52 | 1cmx52 | 1dm52 | 1dmx52 | 1cl52 | 1clx52 | 1dl52 | 1dlx52 |
| -1 | 1cs51 | 1csx51 | 1ds51 | 1dsx51 | 1cm51 | 1cmx51 | 1dm51 | 1dmx51 | 1cl51 | 1clx51 | 1dl51 | 1dlx51 |
| 0 | 1cs50 | 1csx50 | 1ds50 | 1dsx50 | 1cm50 | 1cmx50 | 1dm50 | 1dmx50 | 1cl50 | 1clx50 | 1dl50 | 1dlx50 |
| 1 | 1cs49 | 1csx49 | 1ds49 | 1dsx49 | 1cm49 | 1cmx49 | 1dm49 | 1dmx49 | 1cl49 | 1clx49 | 1dl49 | 1dlx49 |
| 2 | 1cs48 | 1csx48 | 1ds48 | 1dsx48 | 1cm48 | 1cmx48 | 1dm48 | 1dmx48 | 1cl48 | 1clx48 | 1dl48 | 1dlx48 |
| 3 | 1cs47 | 1csx47 | 1ds47 | 1dsx47 | 1cm47 | 1cmx47 | 1dm47 | 1dmx47 | 1cl47 | 1clx47 | 1dl47 | 1dlx47 |
| 4 | 1cs46 | 1csx46 | 1ds46 | 1dsx46 | 1cm46 | 1cmx46 | 1dm46 | 1dmx46 | 1cl46 | 1clx46 | 1dl46 | 1dlx46 |
| 5 | 1cs45 | 1csx45 | 1ds45 | 1dsx45 | 1cm45 | 1cmx45 | 1dm45 | 1dmx45 | 1cl45 | 1clx45 | 1dl45 | 1dlx45 |
| 6 | 1cs44 | 1csx44 | 1ds44 | 1dsx44 | 1cm44 | 1cmx44 | 1dm44 | 1dmx44 | 1cl44 | 1clx44 | 1dl44 | 1dlx44 |
| 7 | 1cs43 | 1csx43 | 1ds43 | 1dsx43 | 1cm43 | 1cmx43 | 1dm43 | 1dmx43 | 1cl43 | 1clx43 | 1dl43 | 1dlx43 |
| 8 | 1cs42 | 1csx42 | 1ds42 | 1dsx42 | 1cm42 | 1cmx42 | 1dm42 | 1dmx42 | 1cl42 | 1clx42 | 1dl42 | 1dlx42 |
| 9 | 1cs41 | 1csx41 | 1ds41 | 1dsx41 | 1cm41 | 1cmx41 | 1dm41 | 1dmx41 | 1cl41 | 1clx41 | 1dl41 | 1dlx41 |
| 10 | 1cs40 | 1csx40 | 1ds40 | 1dsx40 | 1cm40 | 1cmx40 | 1dm40 | 1dmx40 | 1cl40 | 1clx40 | 1dl40 | 1dlx40 |
| 11 | 1cs39 | 1csx39 | 1ds39 | 1dsx39 | 1cm39 | 1cmx39 | 1dm39 | 1dmx39 | 1cl39 | 1clx39 | 1dl39 | 1dlx39 |
| 12 | 1cs38 | 1csx38 | 1ds38 | 1dsx38 | 1cm38 | 1cmx38 | 1dm38 | 1dmx38 | 1cl38 | 1clx38 | 1dl38 | 1dlx38 |
| 13 | 1cs37 | 1csx37 | 1ds37 | 1dsx37 | 1cm37 | 1cmx37 | 1dm37 | 1dmx37 | 1cl37 | 1clx37 | 1dl37 | 1dlx37 |
| 14 | 1cs36 | 1csx36 | 1ds36 | 1dsx36 | 1cm36 | 1cmx36 | 1dm36 | 1dmx36 | 1cl36 | 1clx36 | 1dl36 | 1dlx36 |
| 15 | 1cs35 | 1csx35 | 1ds35 | 1dsx35 | 1cm35 | 1cmx35 | 1dm35 | 1dmx35 | 1cl35 | 1clx35 | 1dl35 | 1dlx35 |
| 16 | 1cs34 | 1csx34 | 1ds34 | 1dsx34 | 1cm34 | 1cmx34 | 1dm34 | 1dmx34 | 1cl34 | 1clx34 | 1dl34 | 1dlx34 |
| 17 | 1cs33 | 1csx33 | 1ds33 | 1dsx33 | 1cm33 | 1cmx33 | 1dm33 | 1dmx33 | 1cl33 | 1clx33 | 1dl33 | 1dlx33 |
| 18 | 1cs32 | 1csx32 | 1ds32 | 1dsx32 | 1cm32 | 1cmx32 | 1dm32 | 1dmx32 | 1cl32 | 1clx32 | 1dl32 | 1dlx32 |
| 19 | 1cs31 | 1csx31 | 1ds31 | 1dsx31 | 1cm31 | 1cmx31 | 1dm31 | 1dmx31 | 1cl31 | 1clx31 | 1dl31 | 1dlx31 |
| 20 | 1cs30 | 1csx30 | 1ds30 | 1dsx30 | 1cm30 | 1cmx30 | 1dm30 | 1dmx30 | 1cl30 | 1clx30 | 1dl30 | 1dlx30 |

Line Names

| Distance From Center of Antenna to Center of Sphere | small conductor at 2 feet | small conductor at 2 feet w/ ant. // | small dialectric at 2 feet | small dialectric at 2 feet w/ ant. // | medium conductor at 2 feet | medium conductor at 2 feet w/ ant. // | medium dialectric at 2 feet | medium dialectric at 2 feet w/ ant. // | large conductor at 2 feet | large conductor at 2 feet w/ ant. // | large dialectric at 2 feet | large dialectric at 2 feet w/ ant. // |
|---|---|---|---|---|---|---|---|---|---|---|---|---|
| -20 | 2cs70 | 2csx70 | 2ds70 | 2dsx70 | 2cm70 | 2cmx70 | 2dm70 | 2dmx70 | 2cl70 | 2clx70 | 2dl70 | 2dlx70 |
| -18 | 2cs68 | 2csx68 | 2ds68 | 2dsx68 | 2cm68 | 2cmx68 | 2dm68 | 2dmx68 | 2cl68 | 2clx68 | 2dl68 | 2dlx68 |
| -16 | 2cs66 | 2csx66 | 2ds66 | 2dsx66 | 2cm66 | 2cmx66 | 2dm66 | 2dmx66 | 2cl66 | 2clx66 | 2dl66 | 2dlx66 |
| -14 | 2cs64 | 2csx64 | 2ds64 | 2dsx64 | 2cm64 | 2cmx64 | 2dm64 | 2dmx64 | 2cl64 | 2clx64 | 2dl64 | 2dlx64 |
| -12 | 2cs62 | 2csx62 | 2ds62 | 2dsx62 | 2cm62 | 2cmx62 | 2dm62 | 2dmx62 | 2cl62 | 2clx62 | 2dl62 | 2dlx62 |
| -10 | 2cs60 | 2csx60 | 2ds60 | 2dsx60 | 2cm60 | 2cmx60 | 2dm60 | 2dmx60 | 2cl60 | 2clx60 | 2dl60 | 2dlx60 |
| -8 | 2cs58 | 2csx58 | 2ds58 | 2dsx58 | 2cm58 | 2cmx58 | 2dm58 | 2dmx58 | 2cl58 | 2clx58 | 2dl58 | 2dlx58 |
| -6 | 2cs56 | 2csx56 | 2ds56 | 2dsx56 | 2cm56 | 2cmx56 | 2dm56 | 2dmx56 | 2cl56 | 2clx56 | 2dl56 | 2dlx56 |
| -5 | 2cs55 | 2csx55 | 2ds55 | 2dsx55 | 2cm55 | 2cmx55 | 2dm55 | 2dmx55 | 2cl55 | 2clx55 | 2dl55 | 2dlx55 |
| -4 | 2cs54 | 2csx54 | 2ds54 | 2dsx54 | 2cm54 | 2cmx54 | 2dm54 | 2dmx54 | 2cl54 | 2clx54 | 2dl54 | 2dlx54 |
| -3 | 2cs53 | 2csx53 | 2ds53 | 2dsx53 | 2cm53 | 2cmx53 | 2dm53 | 2dmx53 | 2cl53 | 2clx53 | 2dl53 | 2dlx53 |
| -2 | 2cs52 | 2csx52 | 2ds52 | 2dsx52 | 2cm52 | 2cmx52 | 2dm52 | 2dmx52 | 2cl52 | 2clx52 | 2dl52 | 2dlx52 |
| -1 | 2cs51 | 2csx51 | 2ds51 | 2dsx51 | 2cm51 | 2cmx51 | 2dm51 | 2dmx51 | 2cl51 | 2clx51 | 2dl51 | 2dlx51 |
| 0 | 2cs50 | 2csx50 | 2ds50 | 2dsx50 | 2cm50 | 2cmx50 | 2dm50 | 2dmx50 | 2cl50 | 2clx50 | 2dl50 | 2dlx50 |
| 1 | 2cs49 | 2csx49 | 2ds49 | 2dsx49 | 2cm49 | 2cmx49 | 2dm49 | 2dmx49 | 2cl49 | 2clx49 | 2dl49 | 2dlx49 |
| 2 | 2cs48 | 2csx48 | 2ds48 | 2dsx48 | 2cm48 | 2cmx48 | 2dm48 | 2dmx48 | 2cl48 | 2clx48 | 2dl48 | 2dlx48 |
| 3 | 2cs47 | 2csx47 | 2ds47 | 2dsx47 | 2cm47 | 2cmx47 | 2dm47 | 2dmx47 | 2cl47 | 2clx47 | 2dl47 | 2dlx47 |
| 4 | 2cs46 | 2csx46 | 2ds46 | 2dsx46 | 2cm46 | 2cmx46 | 2dm46 | 2dmx46 | 2cl46 | 2clx46 | 2dl46 | 2dlx46 |
| 5 | 2cs45 | 2csx45 | 2ds45 | 2dsx45 | 2cm45 | 2cmx45 | 2dm45 | 2dmx45 | 2cl45 | 2clx45 | 2dl45 | 2dlx45 |
| 6 | 2cs44 | 2csx44 | 2ds44 | 2dsx44 | 2cm44 | 2cmx44 | 2dm44 | 2dmx44 | 2cl44 | 2clx44 | 2dl44 | 2dlx44 |
| 7 | 2cs43 | 2csx43 | 2ds43 | 2dsx43 | 2cm43 | 2cmx43 | 2dm43 | 2dmx43 | 2cl43 | 2clx43 | 2dl43 | 2dlx43 |
| 8 | 2cs42 | 2csx42 | 2ds42 | 2dsx42 | 2cm42 | 2cmx42 | 2dm42 | 2dmx42 | 2cl42 | 2clx42 | 2dl42 | 2dlx42 |
| 9 | 2cs41 | 2csx41 | 2ds41 | 2dsx41 | 2cm41 | 2cmx41 | 2dm41 | 2dmx41 | 2cl41 | 2clx41 | 2dl41 | 2dlx41 |
| 10 | 2cs40 | 2csx40 | 2ds40 | 2dsx40 | 2cm40 | 2cmx40 | 2dm40 | 2dmx40 | 2cl40 | 2clx40 | 2dl40 | 2dlx40 |
| 11 | 2cs39 | 2csx39 | 2ds39 | 2dsx39 | 2cm39 | 2cmx39 | 2dm39 | 2dmx39 | 2cl39 | 2clx39 | 2dl39 | 2dlx39 |
| 12 | 2cs38 | 2csx38 | 2ds38 | 2dsx38 | 2cm38 | 2cmx38 | 2dm38 | 2dmx38 | 2cl38 | 2clx38 | 2dl38 | 2dlx38 |
| 13 | 2cs37 | 2csx37 | 2ds37 | 2dsx37 | 2cm37 | 2cmx37 | 2dm37 | 2dmx37 | 2cl37 | 2clx37 | 2dl37 | 2dlx37 |
| 14 | 2cs36 | 2csx36 | 2ds36 | 2dsx36 | 2cm36 | 2cmx36 | 2dm36 | 2dmx36 | 2cl36 | 2clx36 | 2dl36 | 2dlx36 |
| 15 | 2cs35 | 2csx35 | 2ds35 | 2dsx35 | 2cm35 | 2cmx35 | 2dm35 | 2dmx35 | 2cl35 | 2clx35 | 2dl35 | 2dlx35 |
| 16 | 2cs34 | 2csx34 | 2ds34 | 2dsx34 | 2cm34 | 2cmx34 | 2dm34 | 2dmx34 | 2cl34 | 2clx34 | 2dl34 | 2dlx34 |
| 17 | 2cs33 | 2csx33 | 2ds33 | 2dsx33 | 2cm33 | 2cmx33 | 2dm33 | 2dmx33 | 2cl33 | 2clx33 | 2dl33 | 2dlx33 |
| 18 | 2cs32 | 2csx32 | 2ds32 | 2dsx32 | 2cm32 | 2cmx32 | 2dm32 | 2dmx32 | 2cl32 | 2clx32 | 2dl32 | 2dlx32 |
| 19 | 2cs31 | 2csx31 | 2ds31 | 2dsx31 | 2cm31 | 2cmx31 | 2dm31 | 2dmx31 | 2cl31 | 2clx31 | 2dl31 | 2dlx31 |
| 20 | 2cs30 | 2csx30 | 2ds30 | 2dsx30 | 2cm30 | 2cmx30 | 2dm30 | 2dmx30 | 2cl30 | 2clx30 | 2dl30 | 2dlx30 |

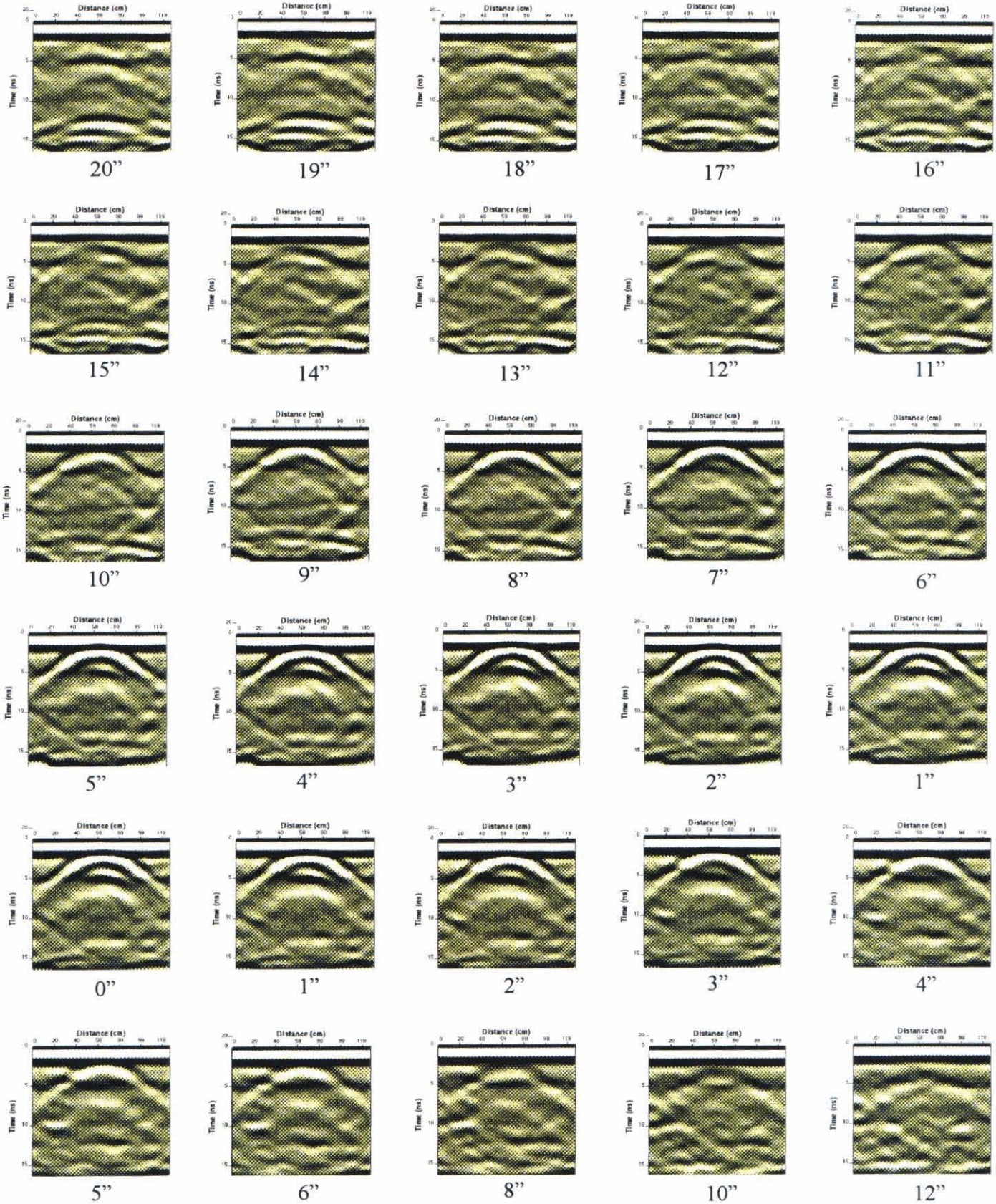


# 1cl: large conductor at 1 foot

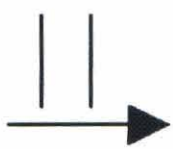

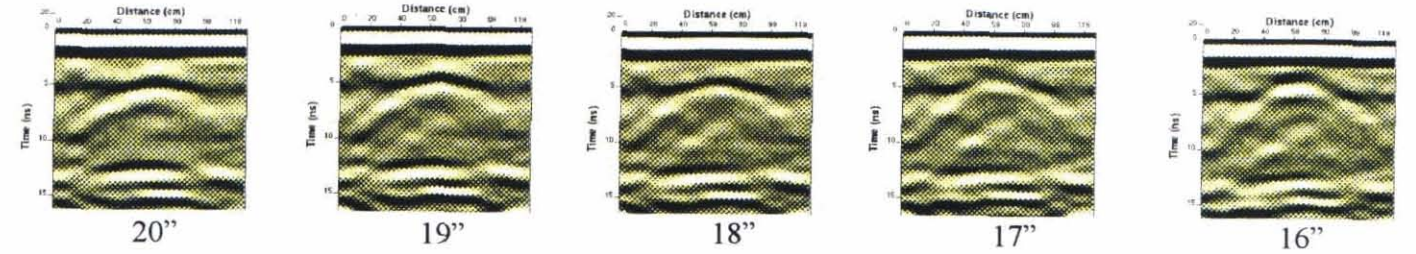


20" 19" 18" 17" 16"

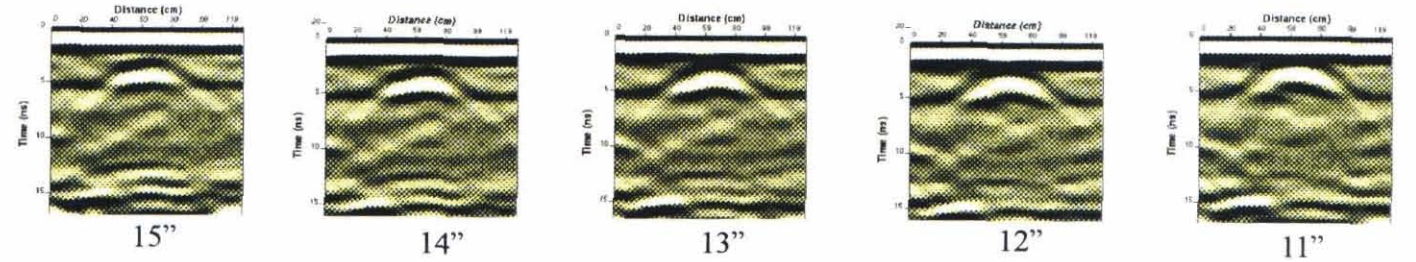


15" 14" 13" 12" 11"

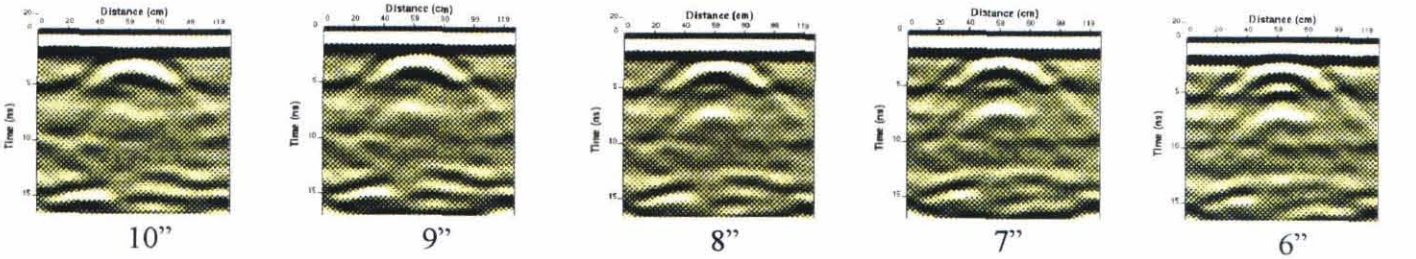


10" 9" 8" 7" 6"

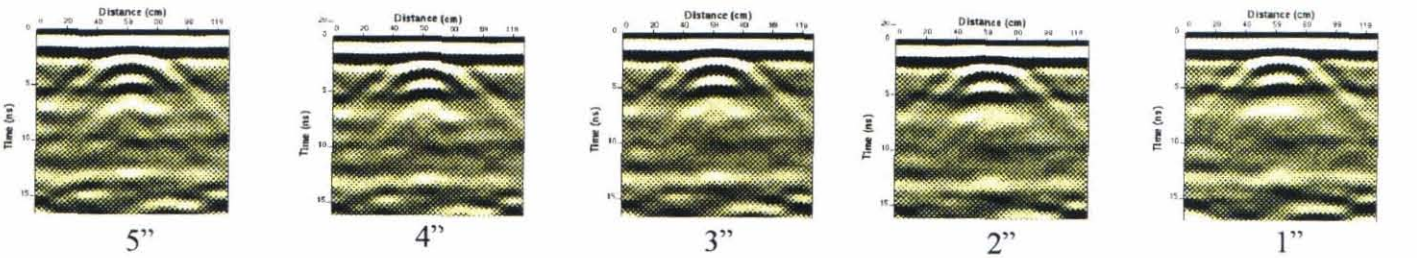


5" 4" 3" 2" 1"

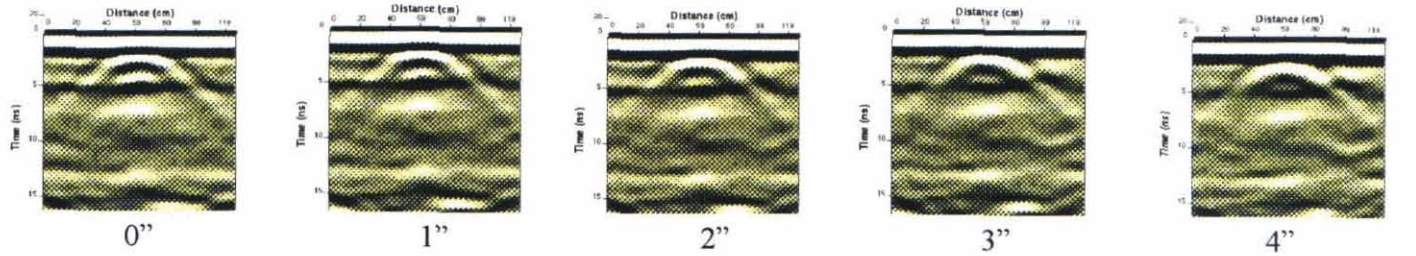


0" 1" 2" 3" 4"

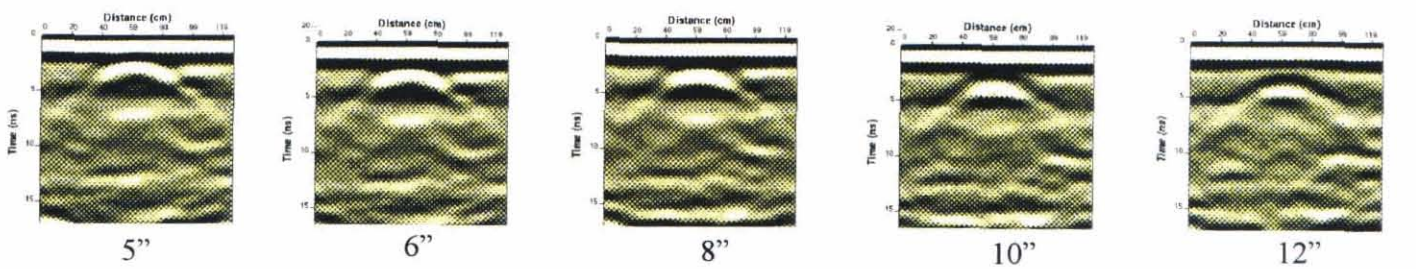


5" 6" 8" 10" 12"

1clx: large conductor at 1 foot

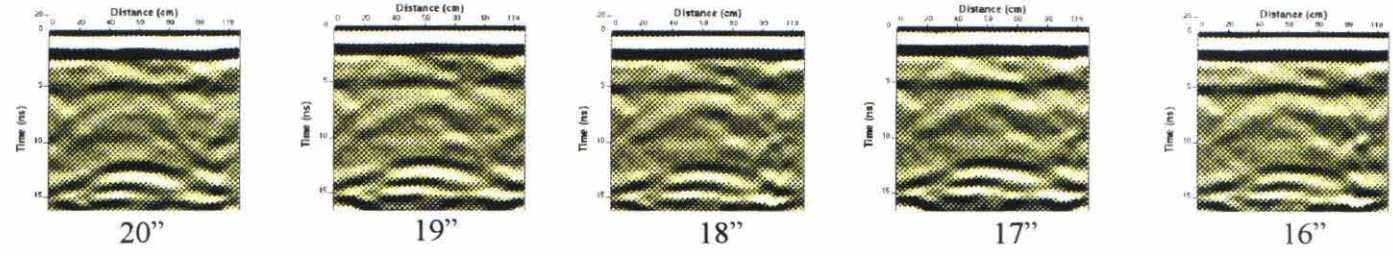


20” 19” 18” 17” 16”

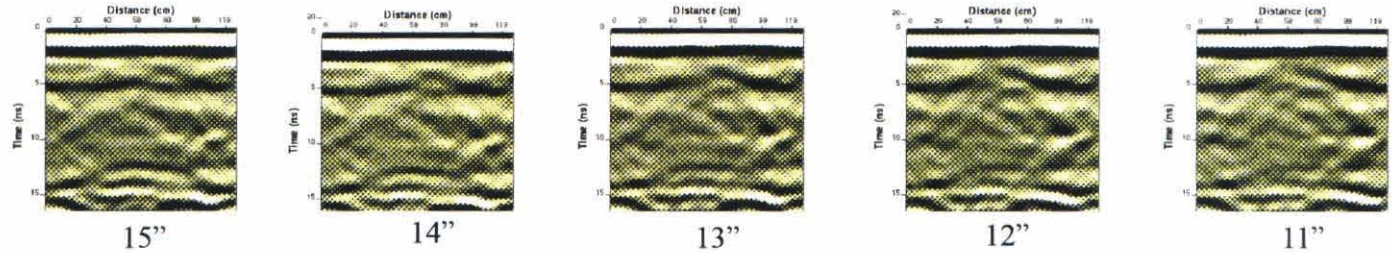


15” 14” 13” 12” 11”

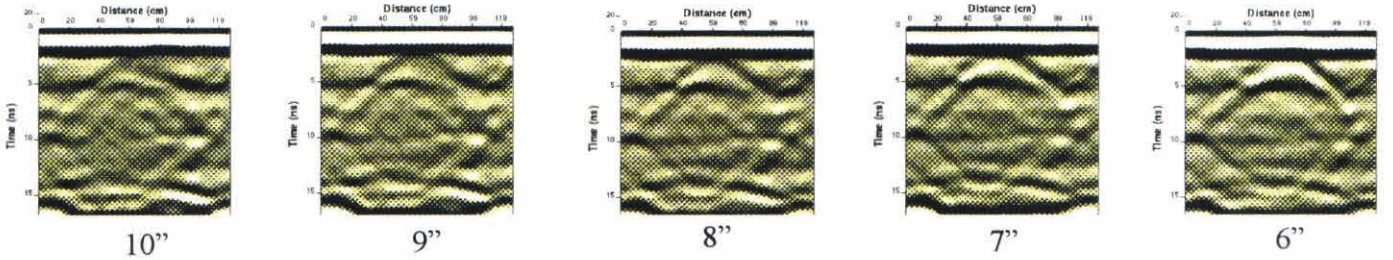


10” 9” 8” 7” 6”

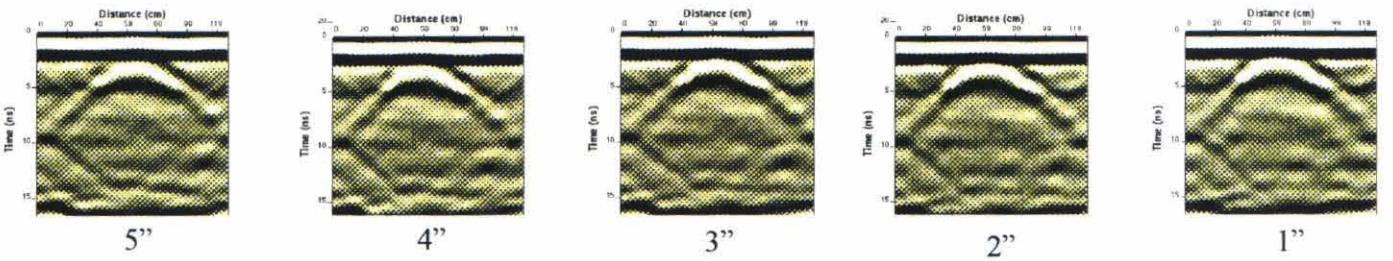


5” 4” 3” 2” 1”

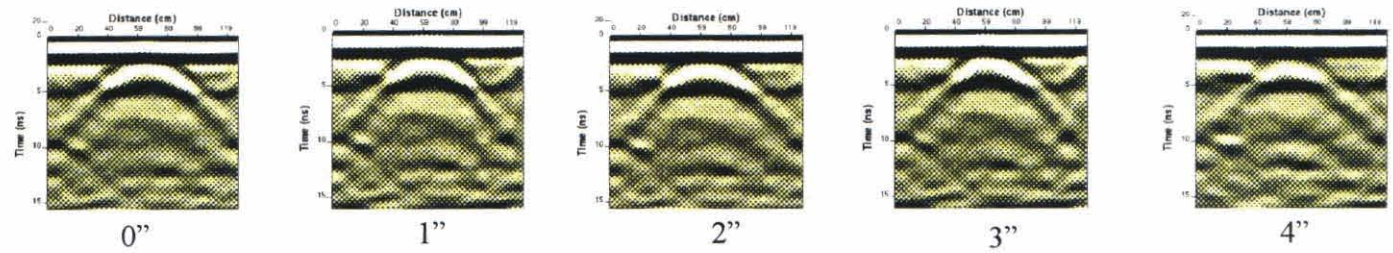


0” 1” 2” 3” 4”

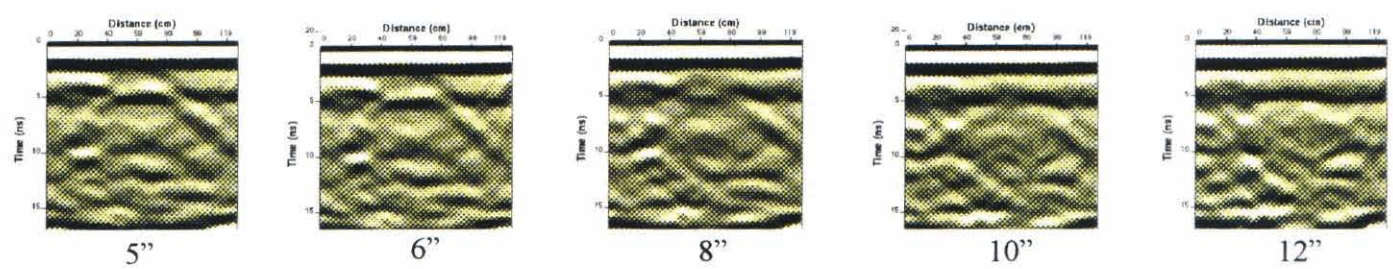


5” 6” 8” 10” 12”

1cm: medium conductor at 1 foot

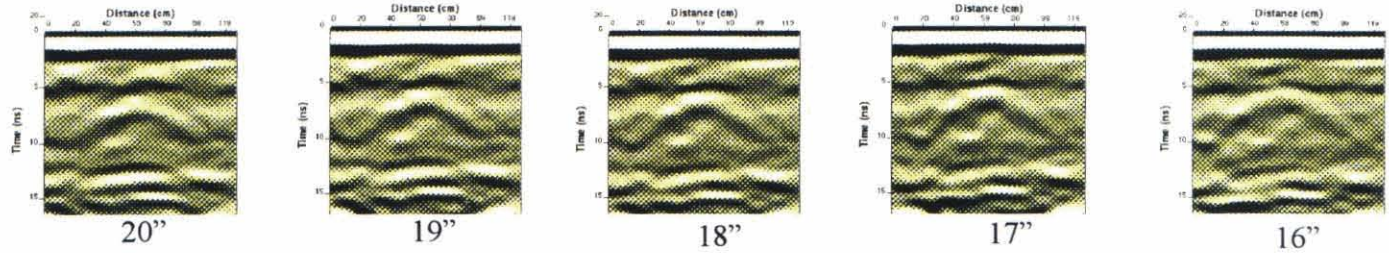


20" 19" 18" 17" 16"

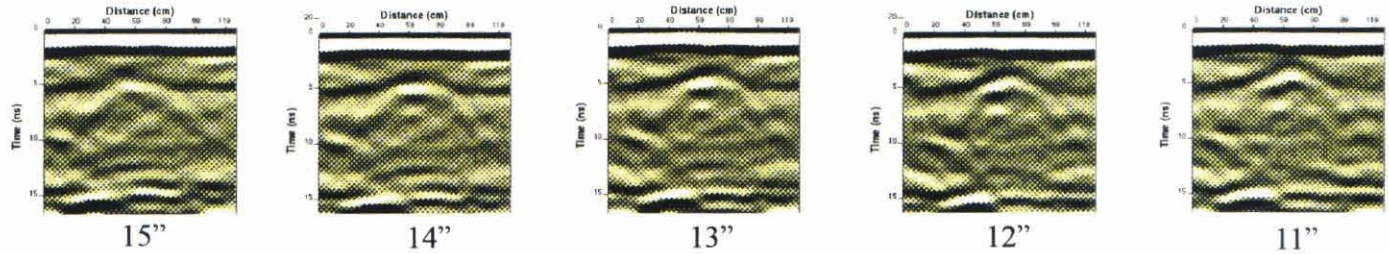


15" 14" 13" 12" 11"

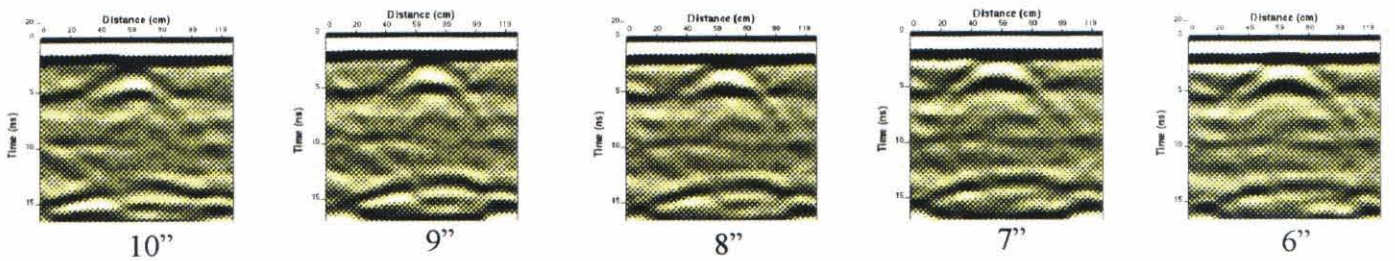


10" 9" 8" 7" 6"

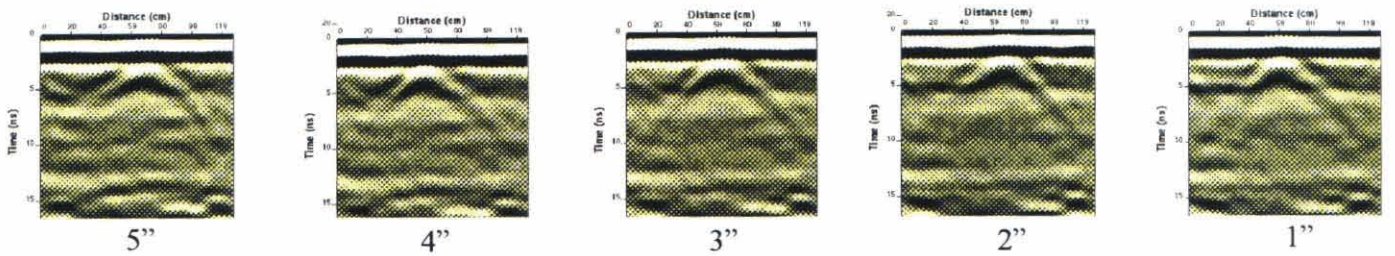


5" 4" 3" 2" 1"

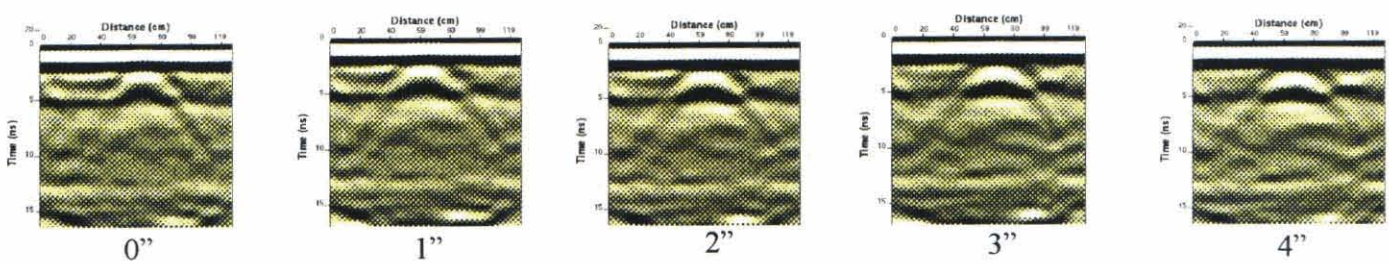


0" 1" 2" 3" 4"

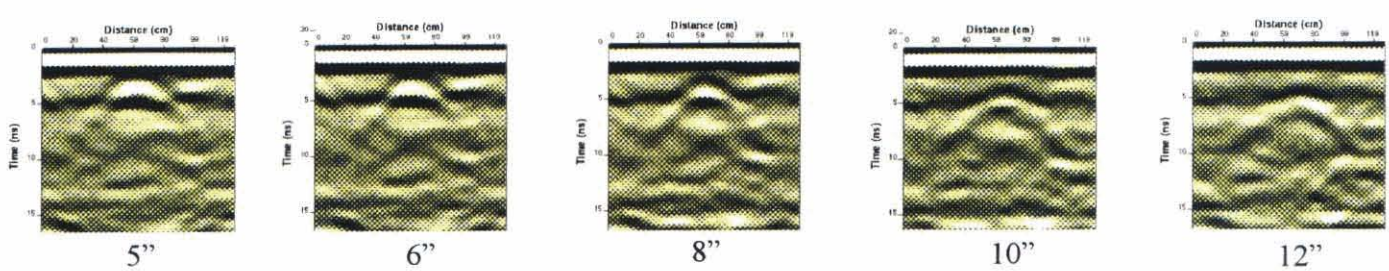


5" 6" 8" 10" 12"

1cmx: medium conductor at 1 foot

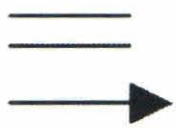

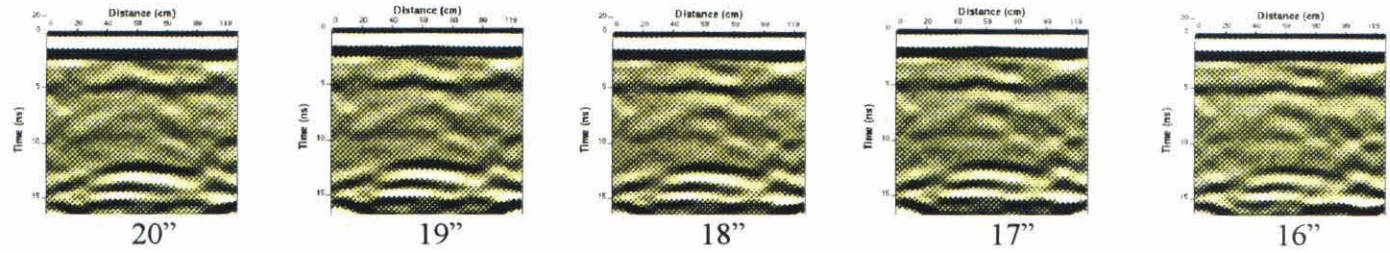


20” 19” 18” 17” 16”

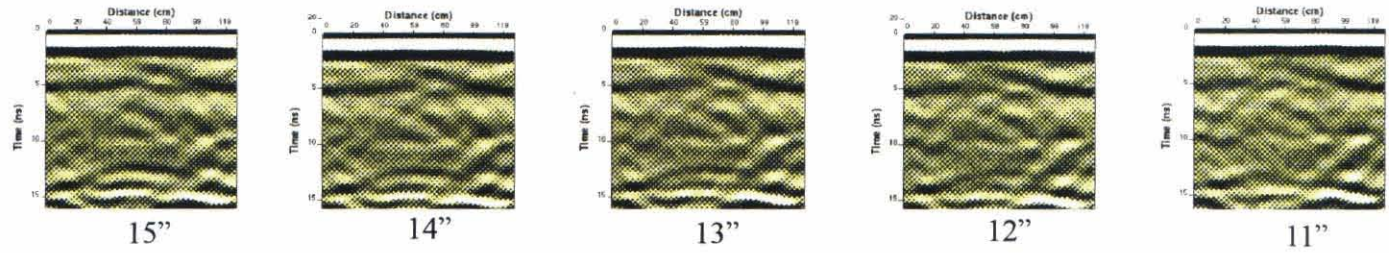


15” 14” 13” 12” 11”

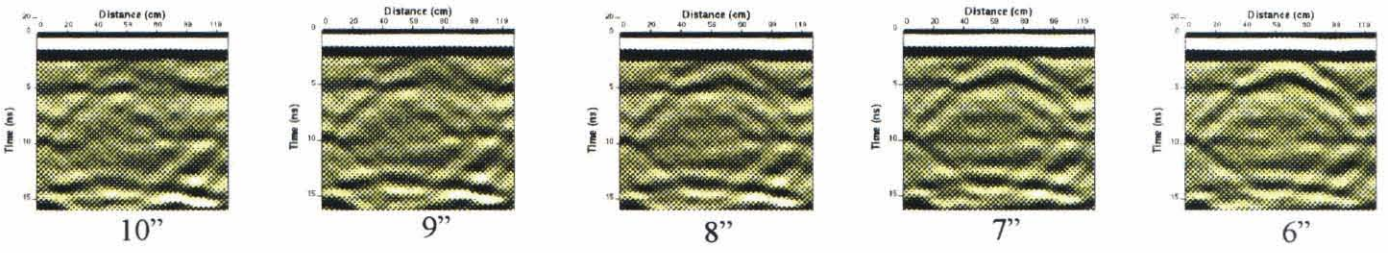


10” 9” 8” 7” 6”

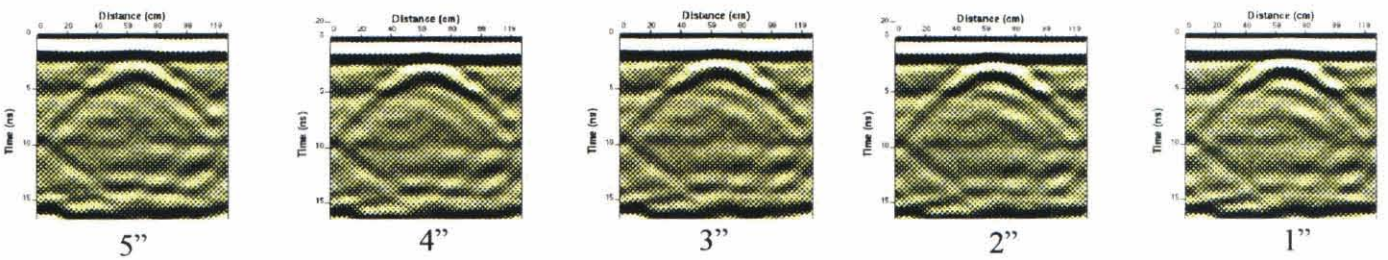


5” 4” 3” 2” 1”

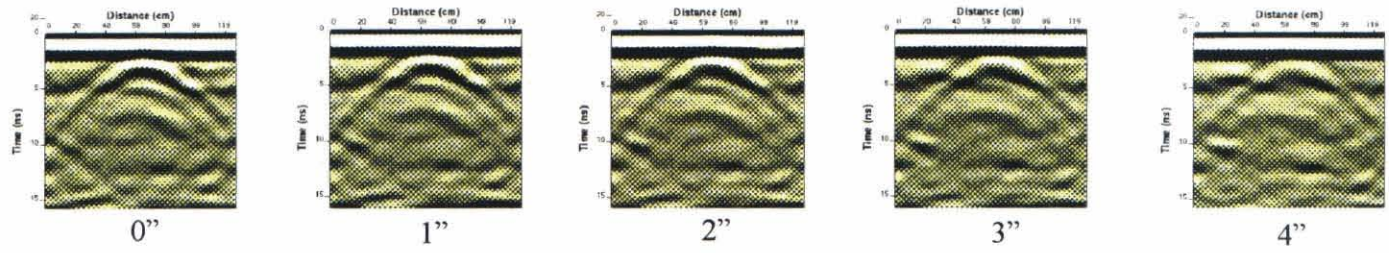


0” 1” 2” 3” 4”

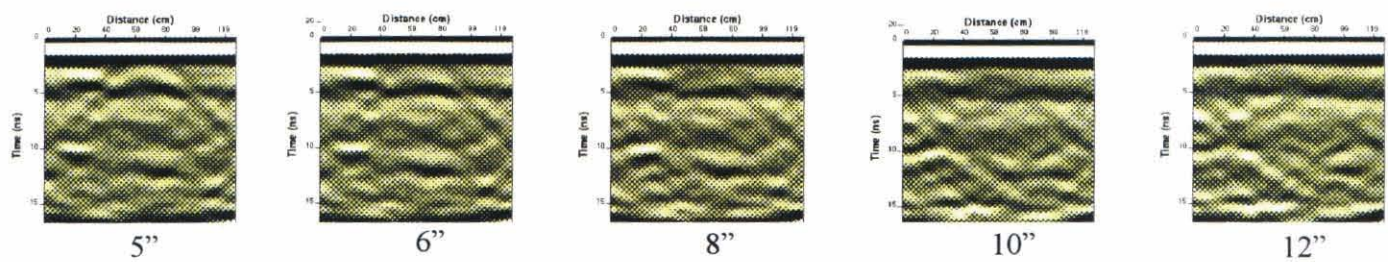


5” 6” 8” 10” 12”

1cs: small conductor at 1 foot

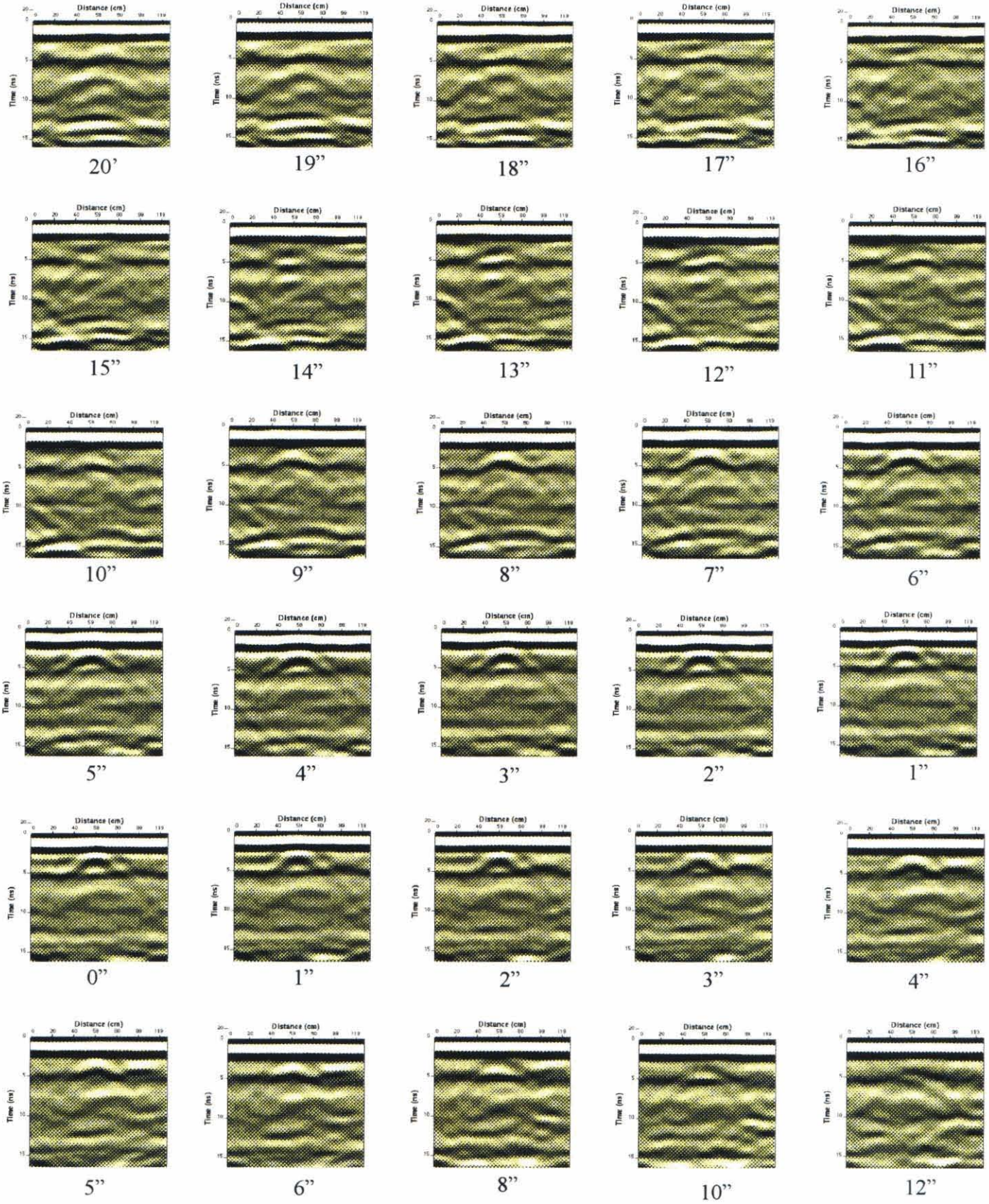


1csx: small conductor at 1 foot

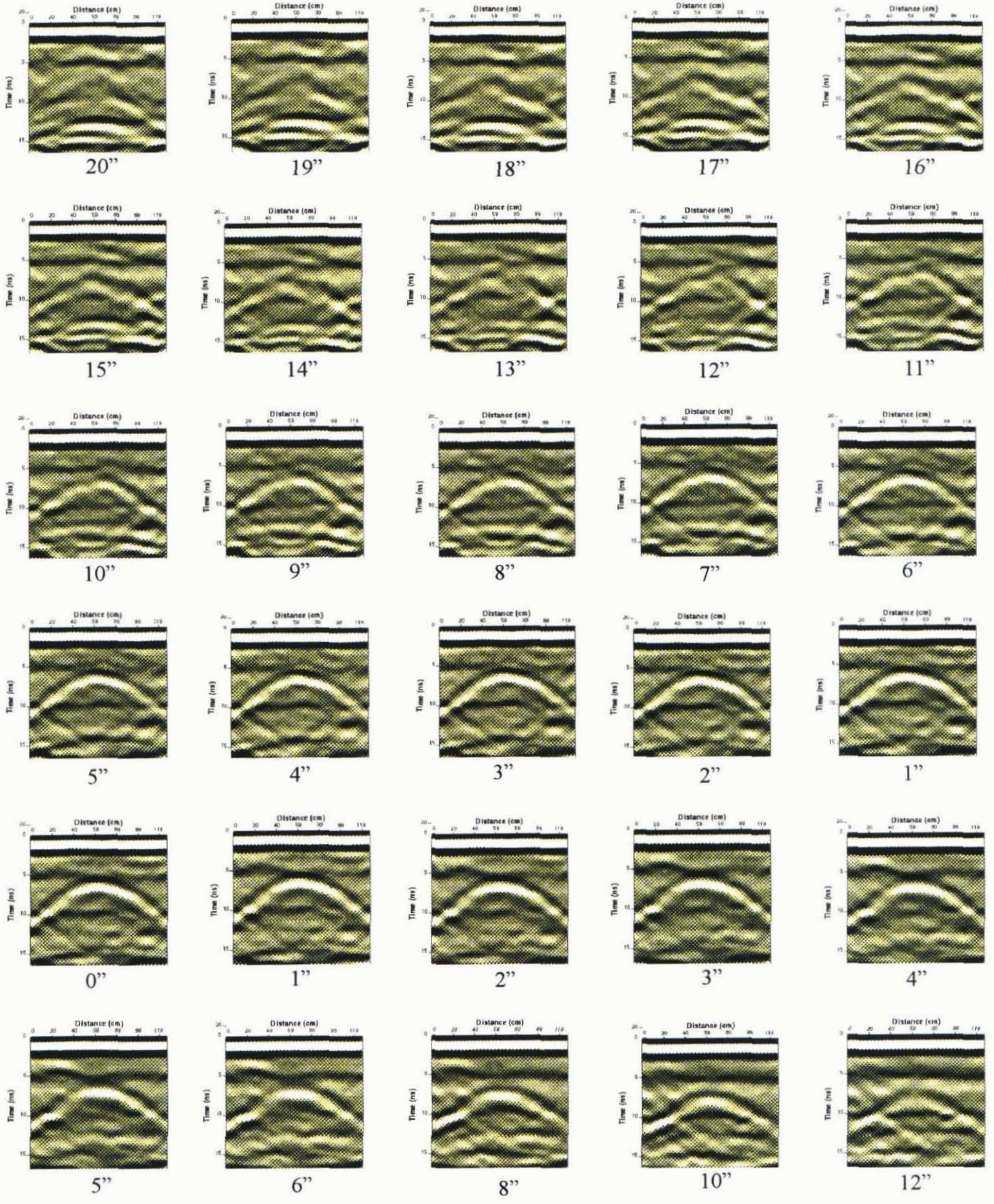


# 2cl: large conductor at 2 feet

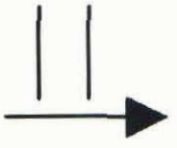

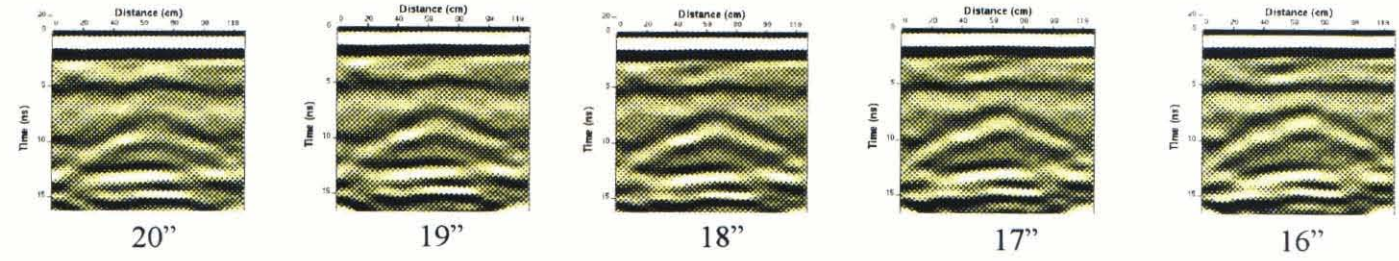


20” 19” 18” 17” 16”

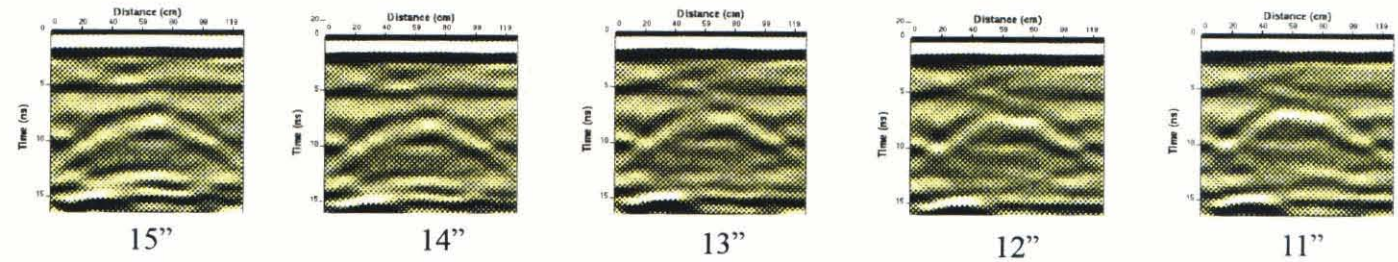


15” 14” 13” 12” 11”

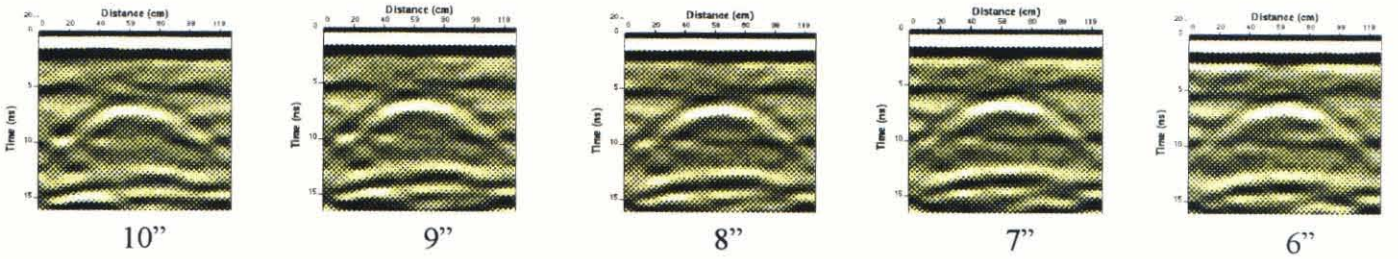


10” 9” 8” 7” 6”

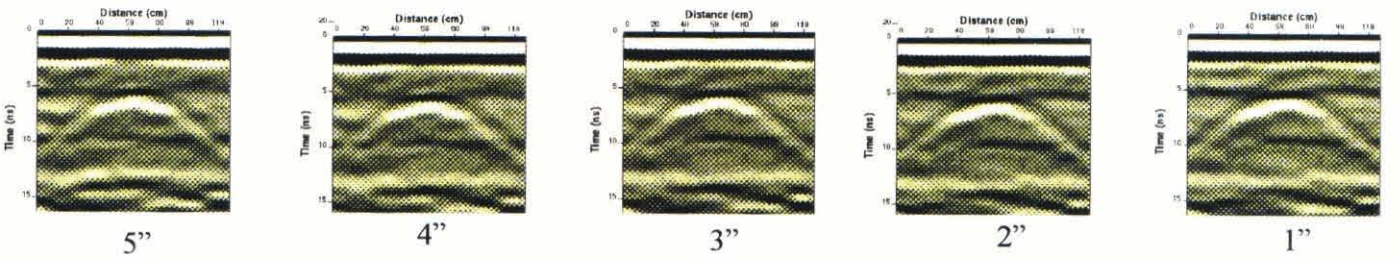


5” 4” 3” 2” 1”

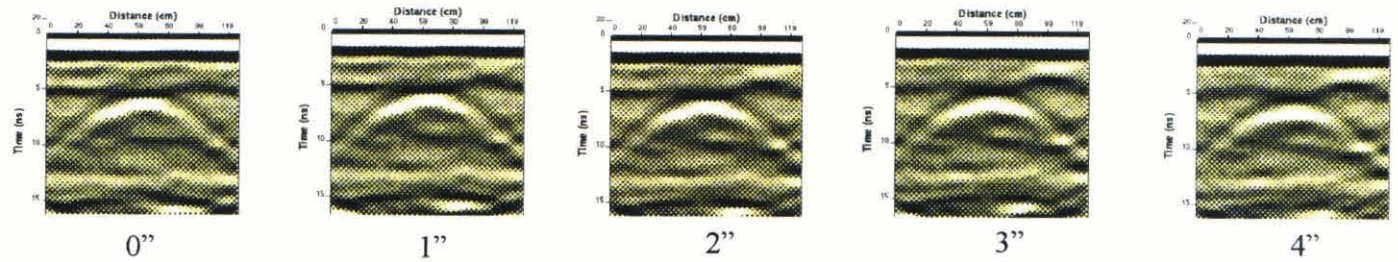


0” 1” 2” 3” 4”

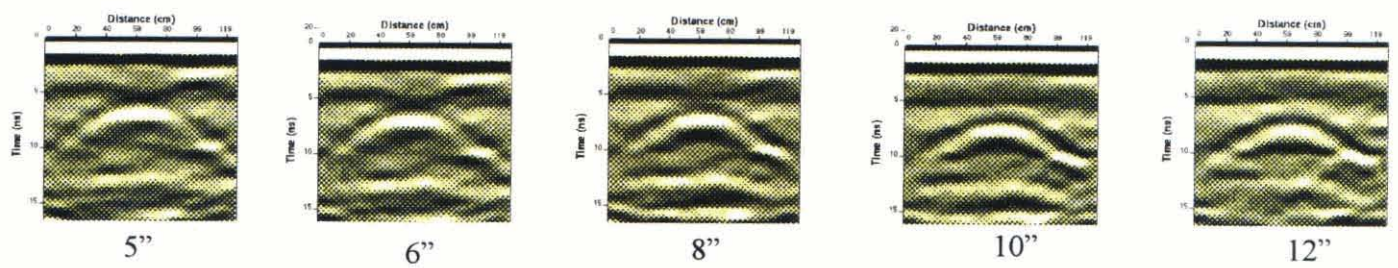


5” 6” 8” 10” 12”

# 2clx: large conductor at 2 feet

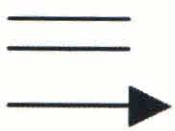


2cm: medium conductor at 2 feet

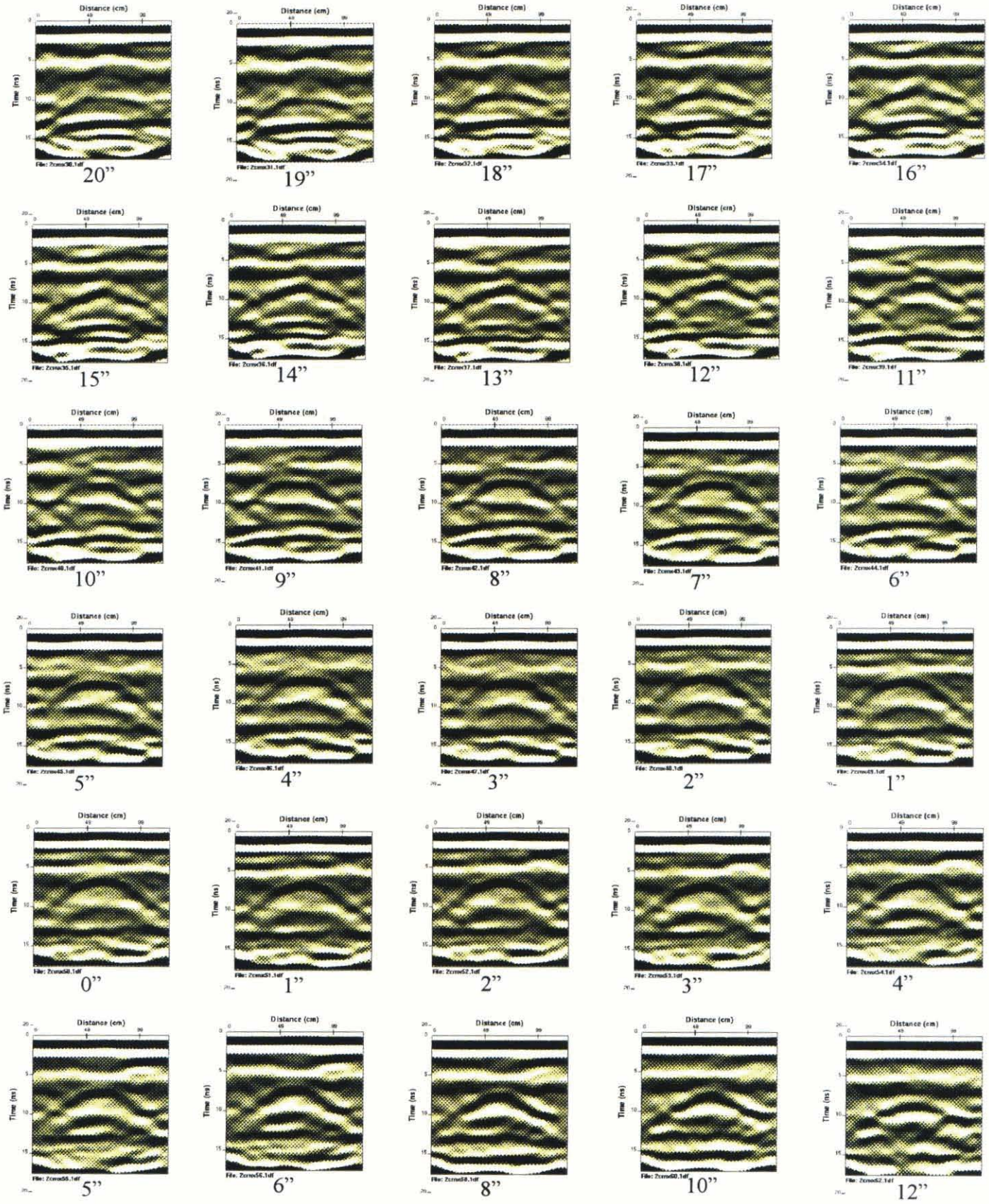


2cmx: medium conductor at 2 feet


2cs: small conductor buried at 2 feet.

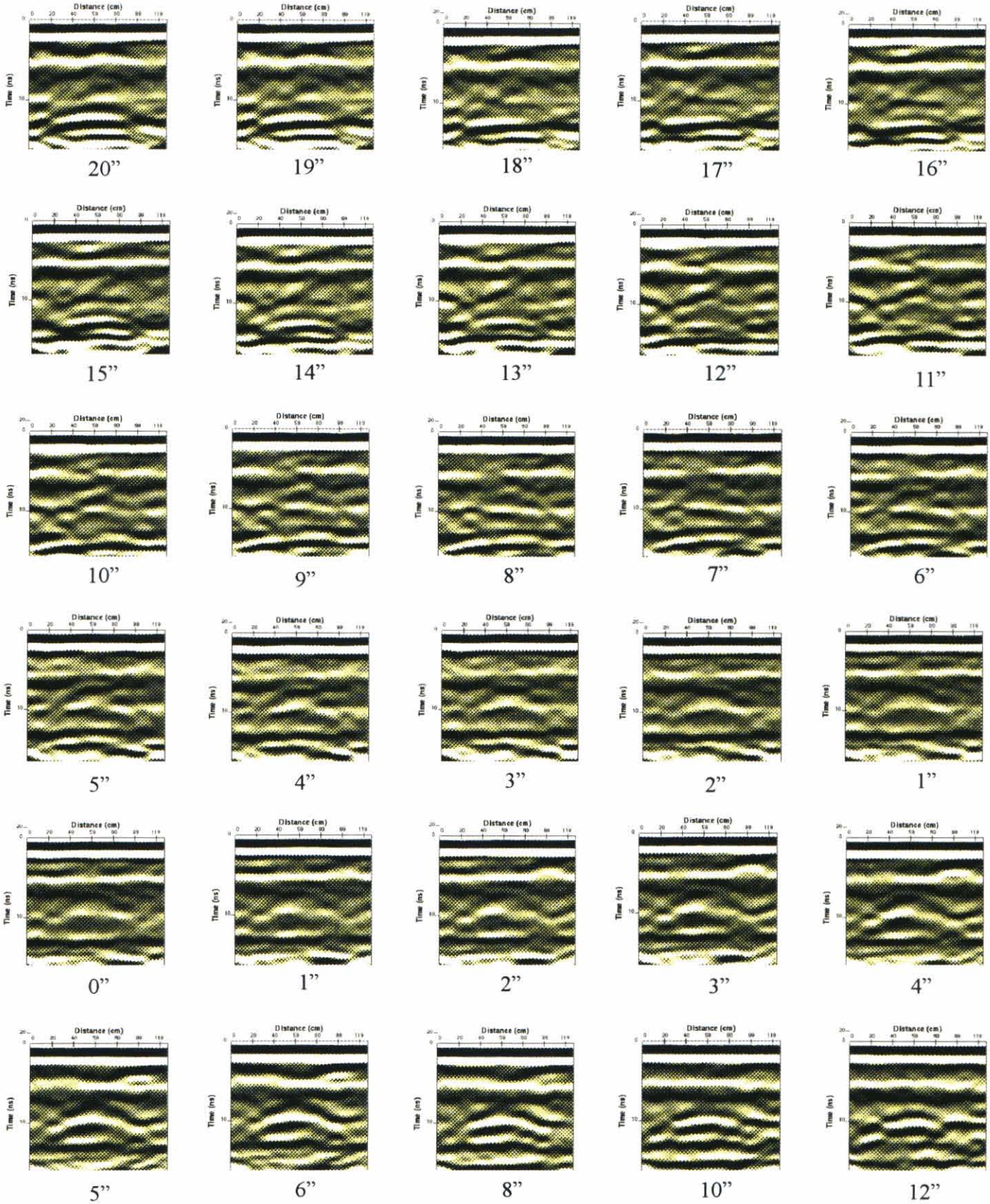


2csx: Small conductor buried at 2 feet.

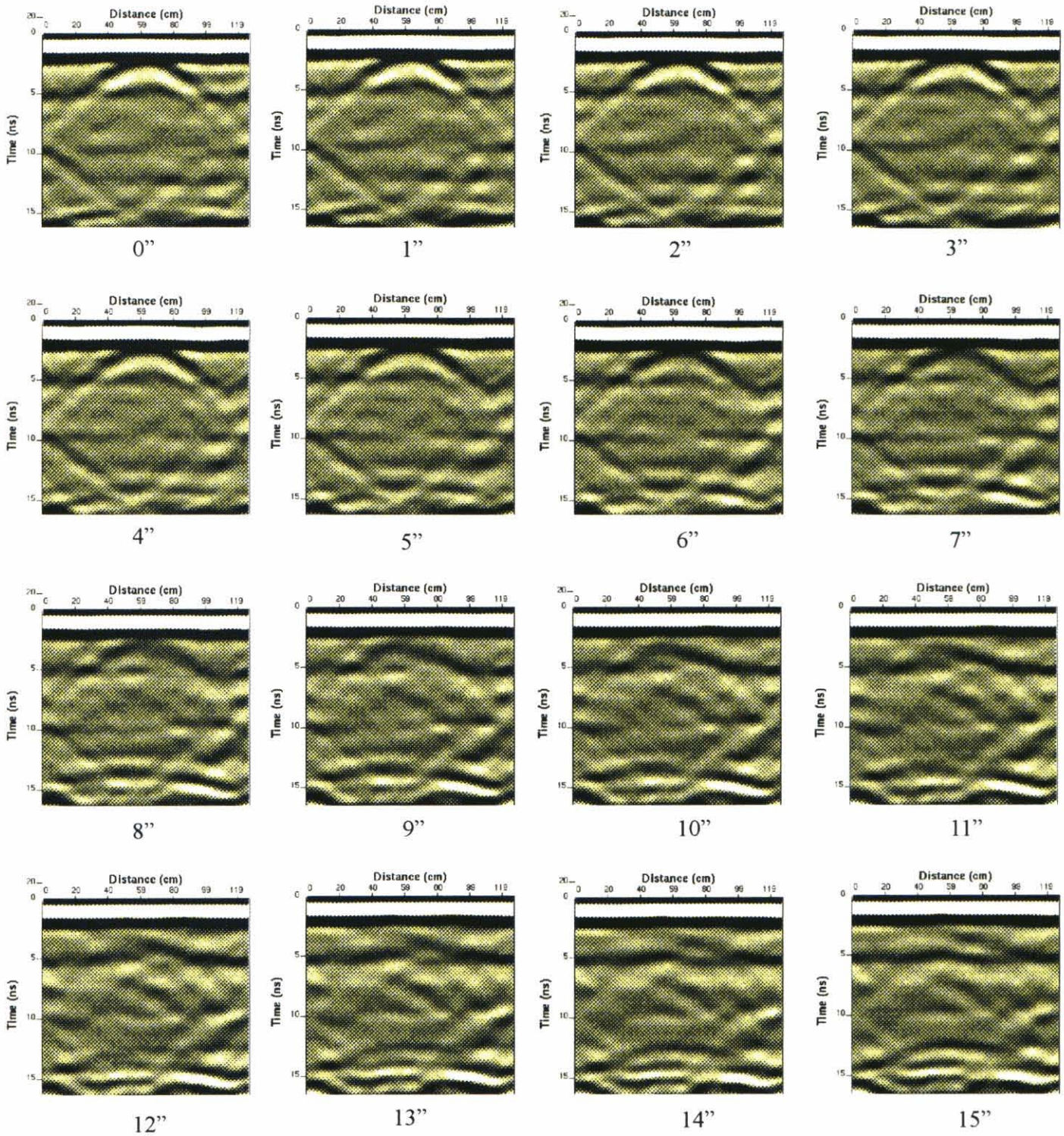


1dl: Large dielectric buried at 1 foot.

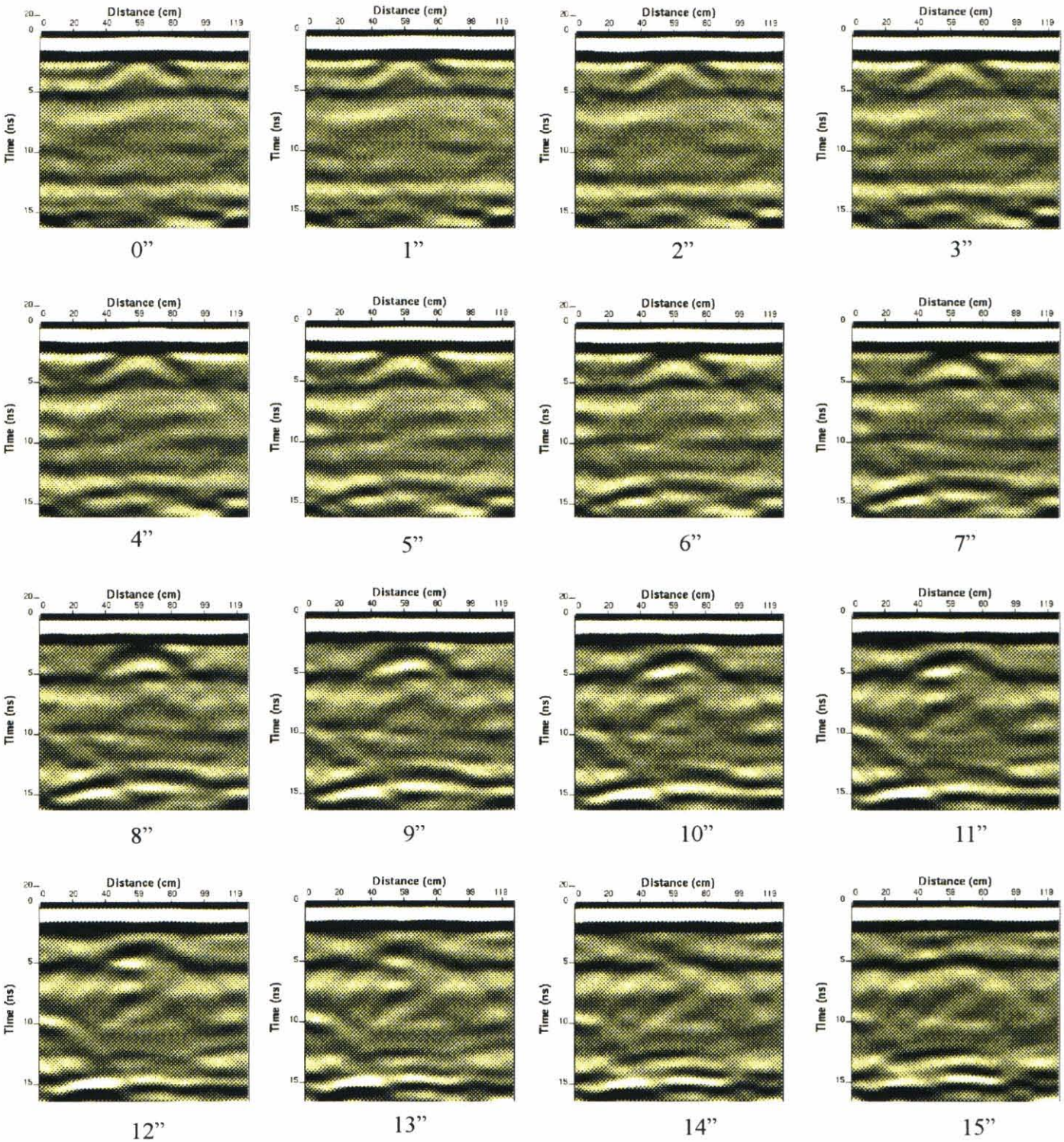


1dlx: Large dielectric buried at 1 foot.

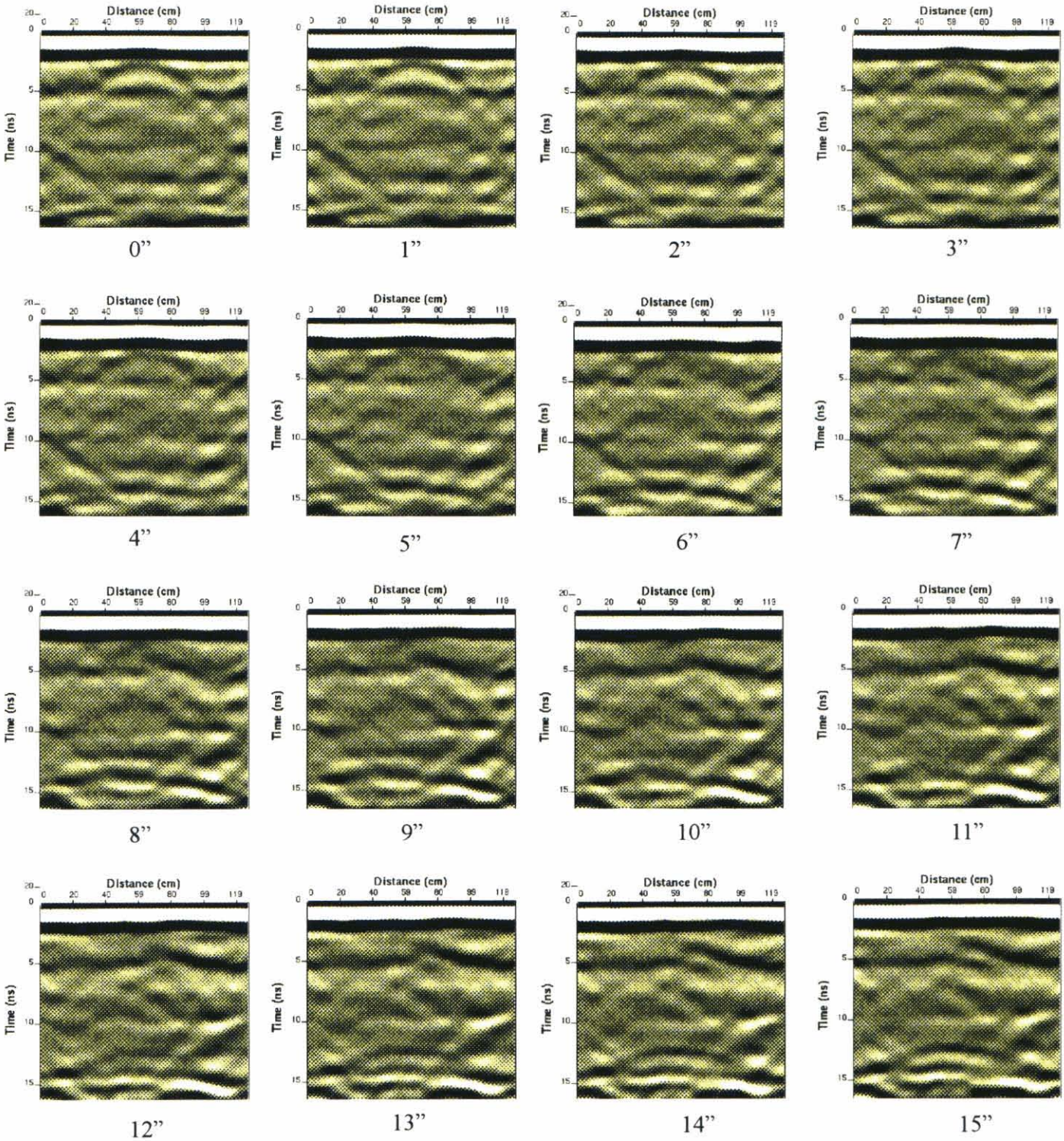


1dm: Medium dielectric buried at 1 foot.

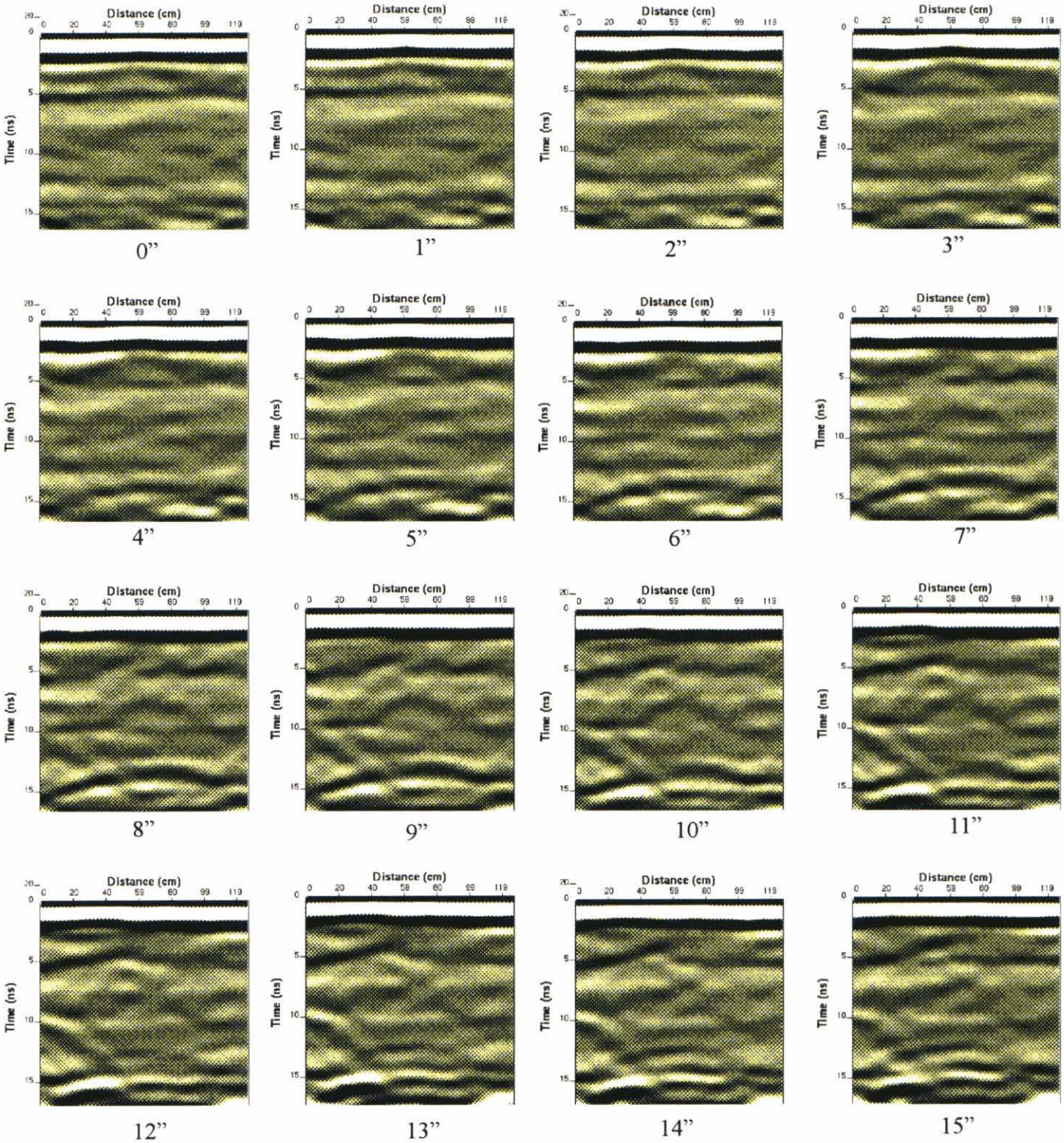


1dmx: Medium dielectric buried at 1 foot

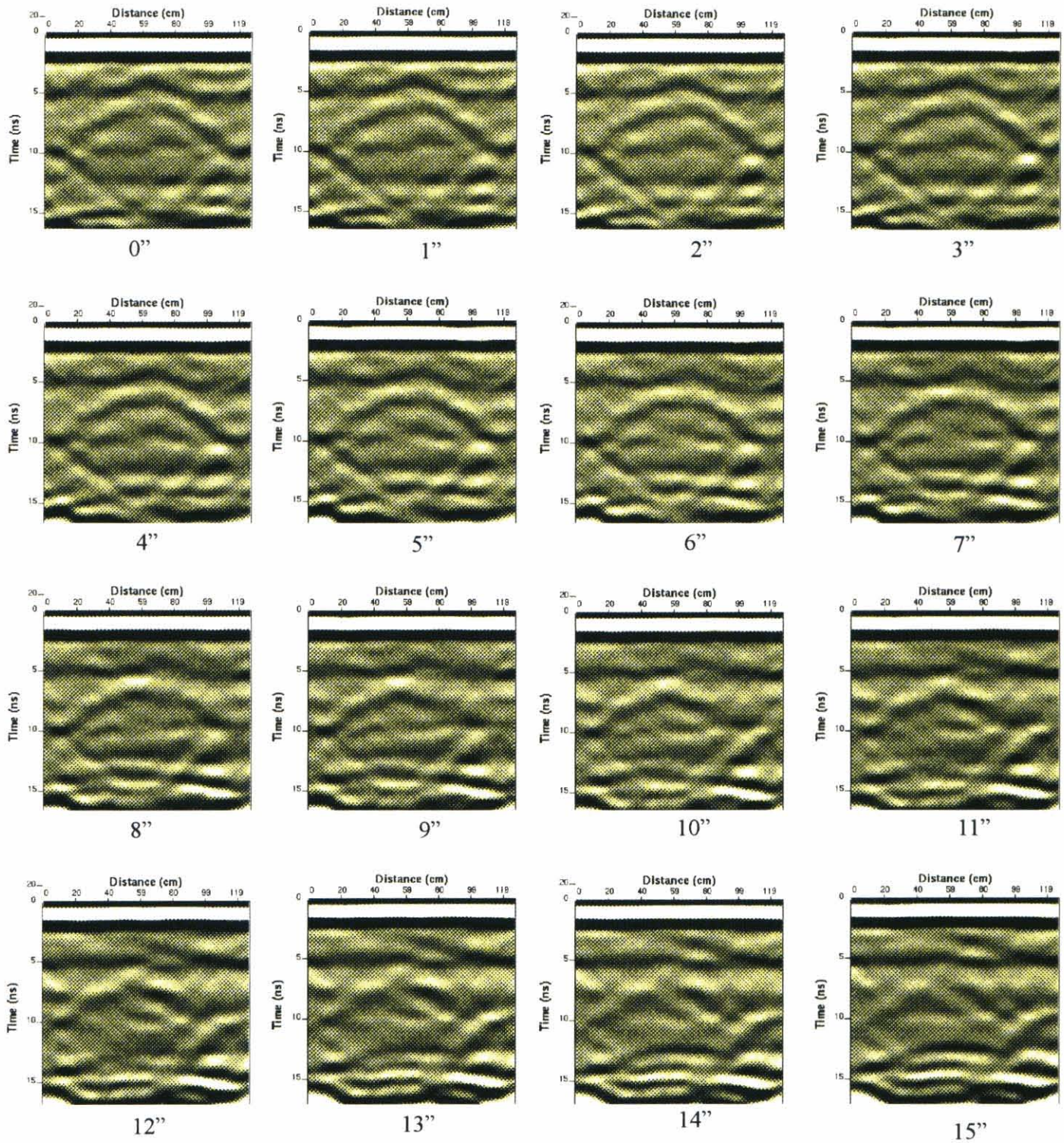


2dl: Large dielectric buried at 2 feet.

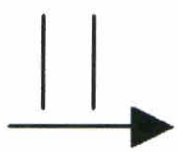

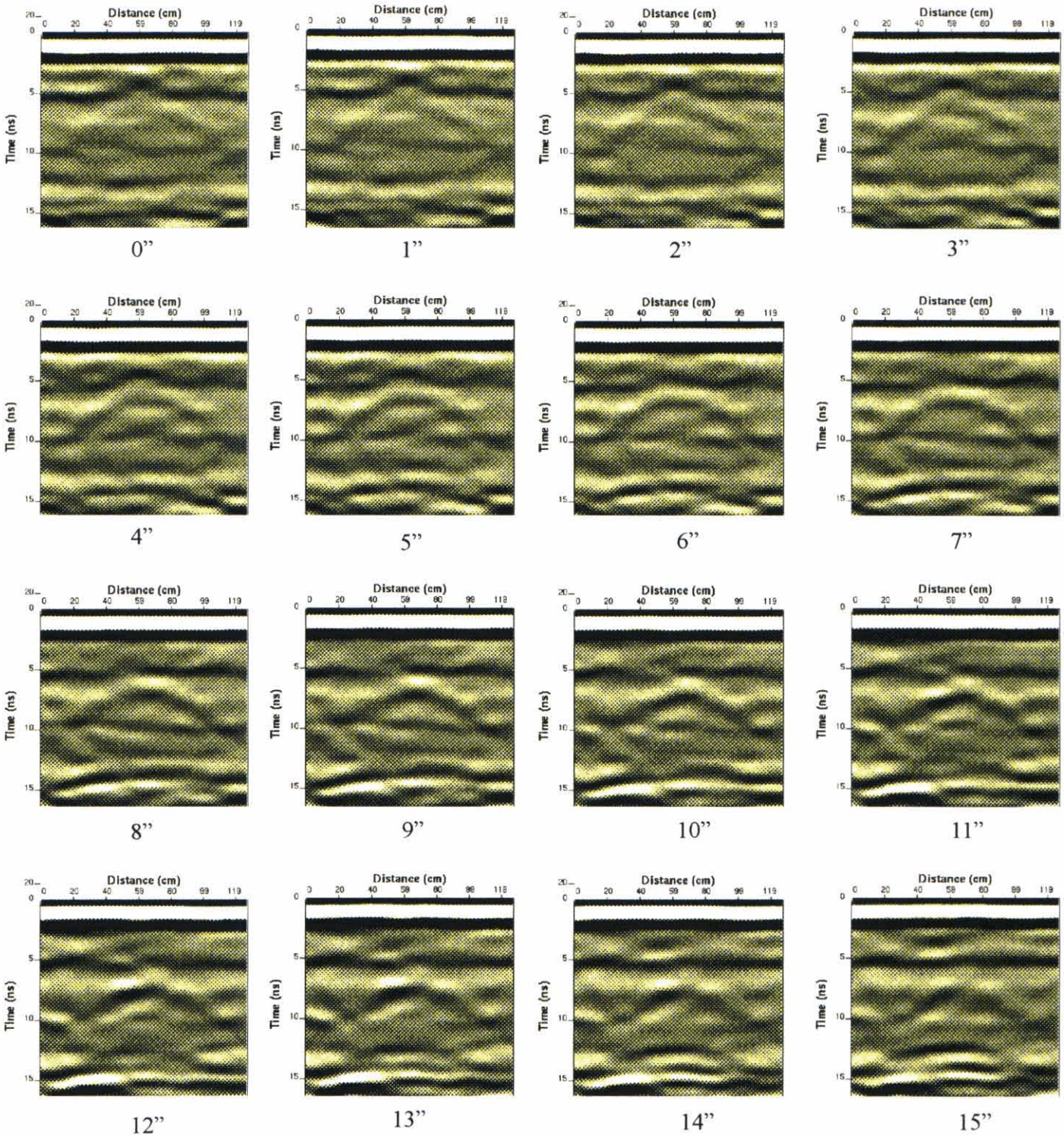


2dlx: Large dielectric buried at 2 feet.

Appendix C

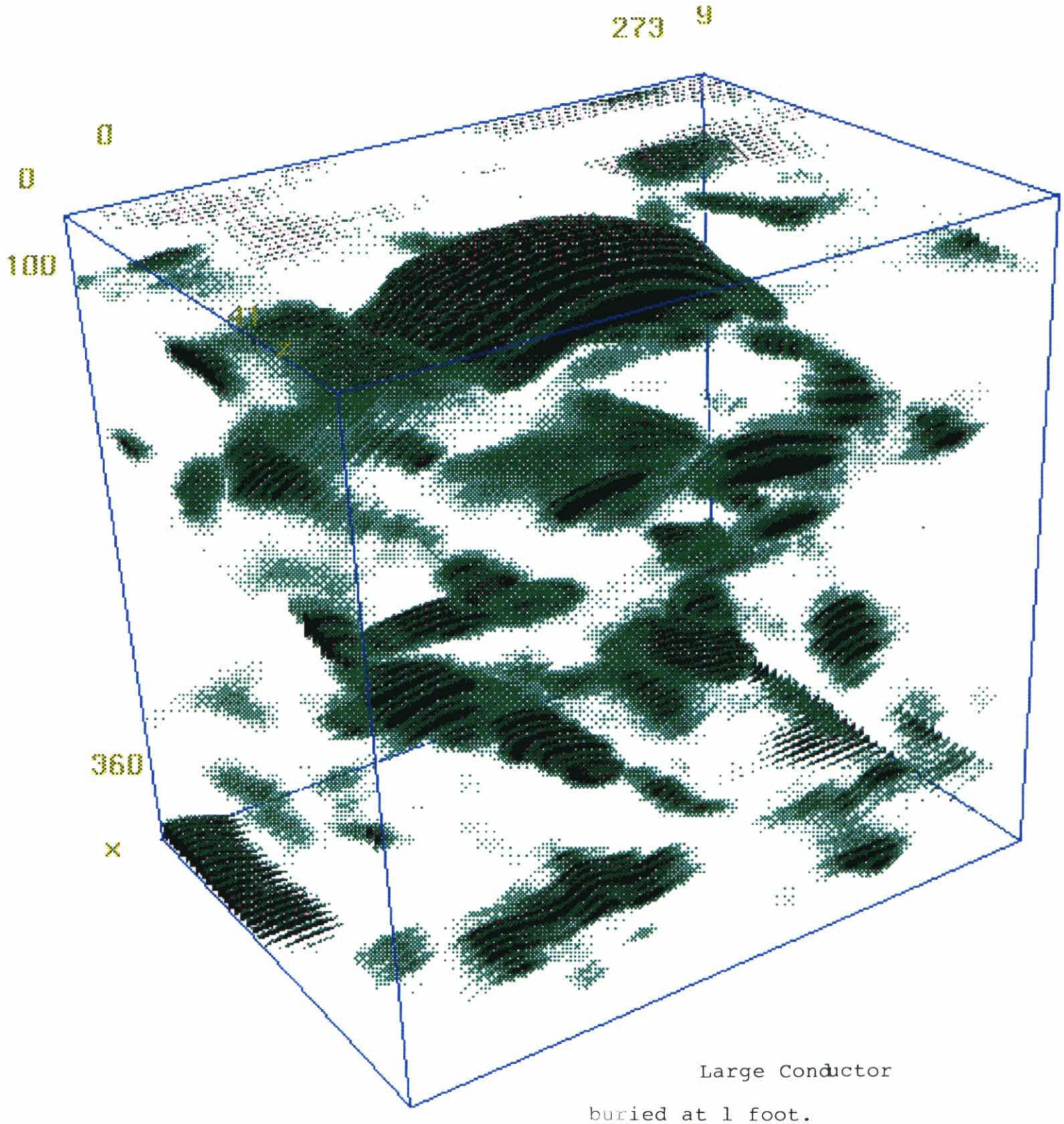


Large Conductor

buried at 1 foot.

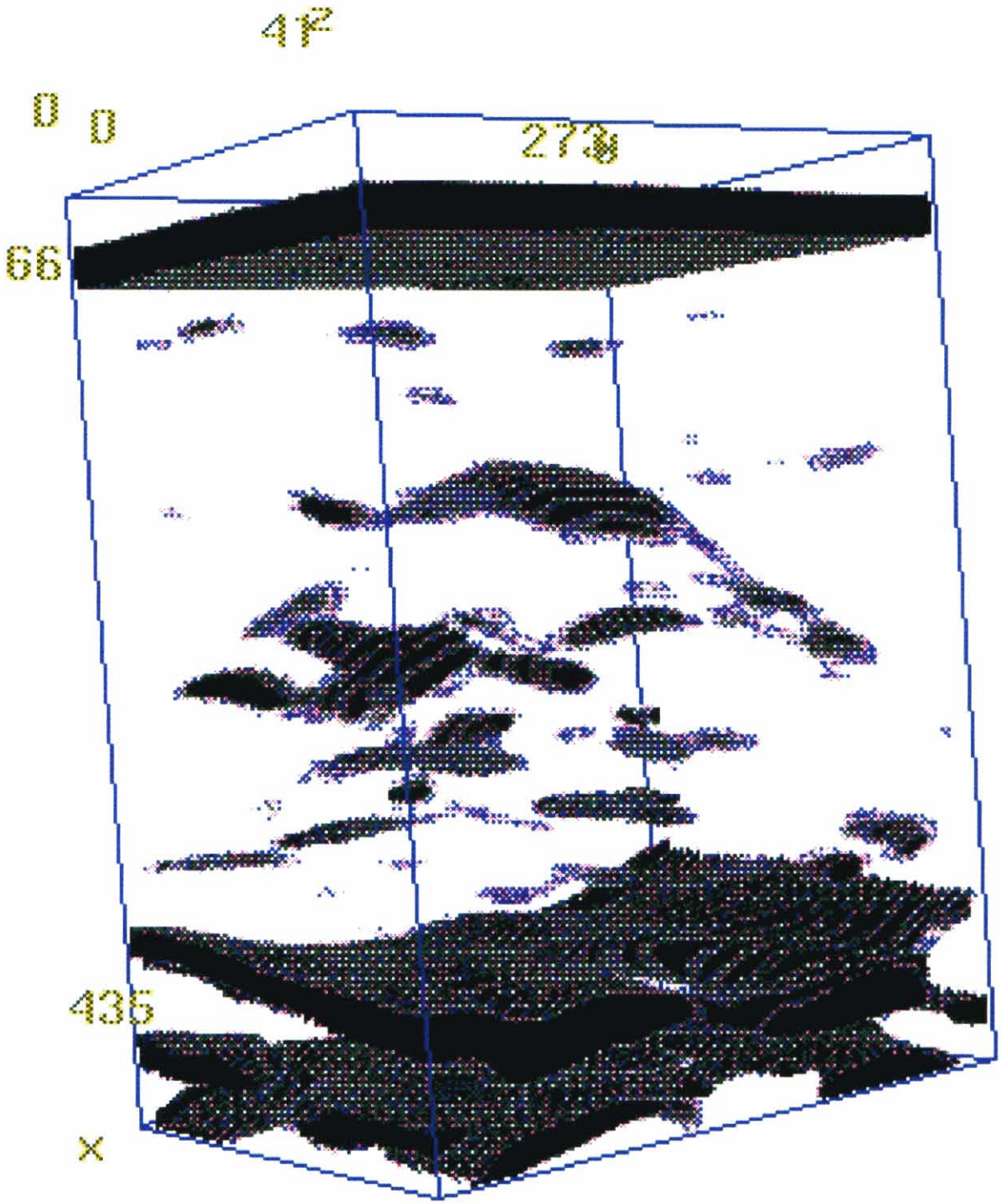


Large conductor buried at 2 feet.

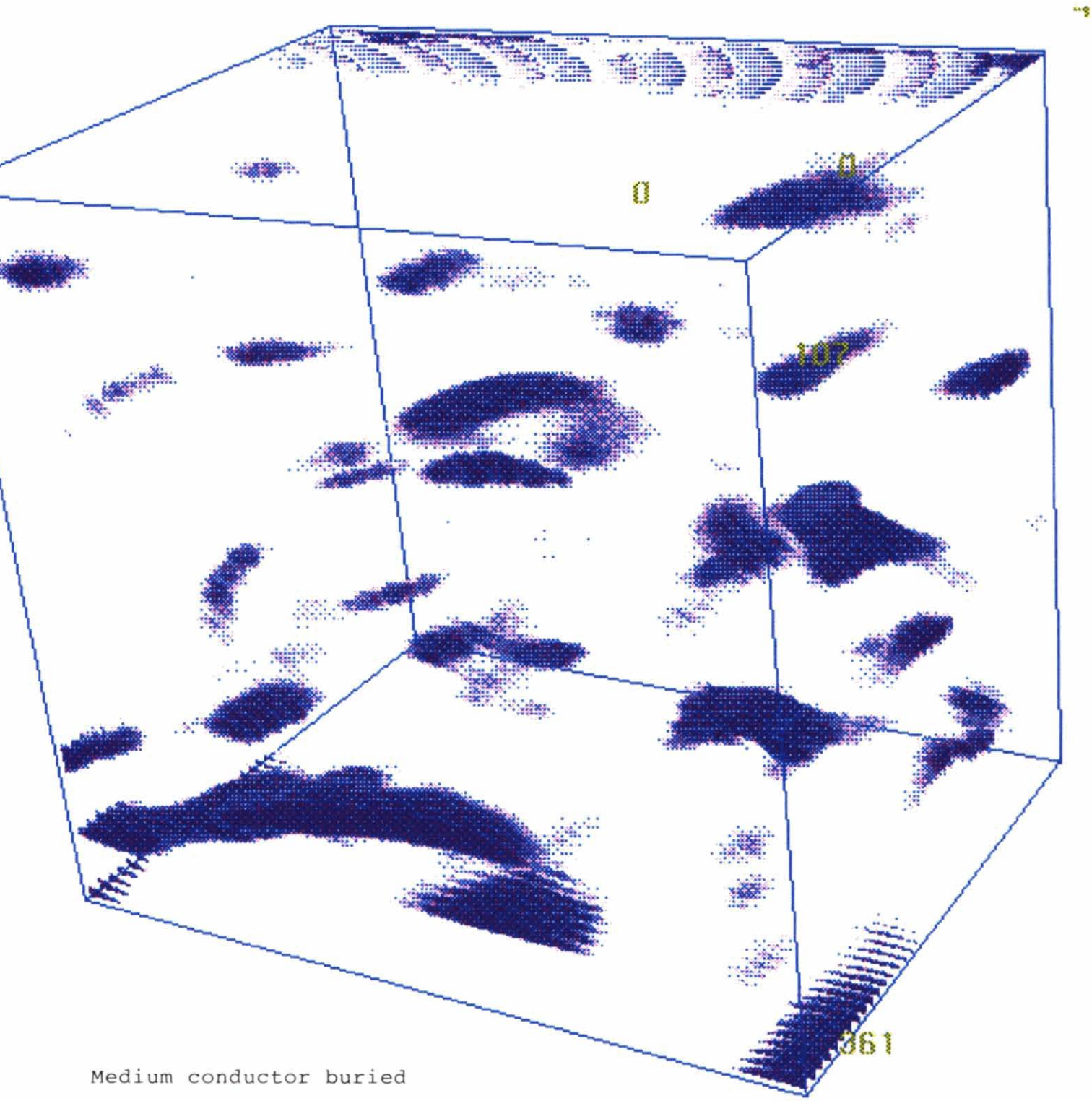


Medium conductor buried
at 2 feet.

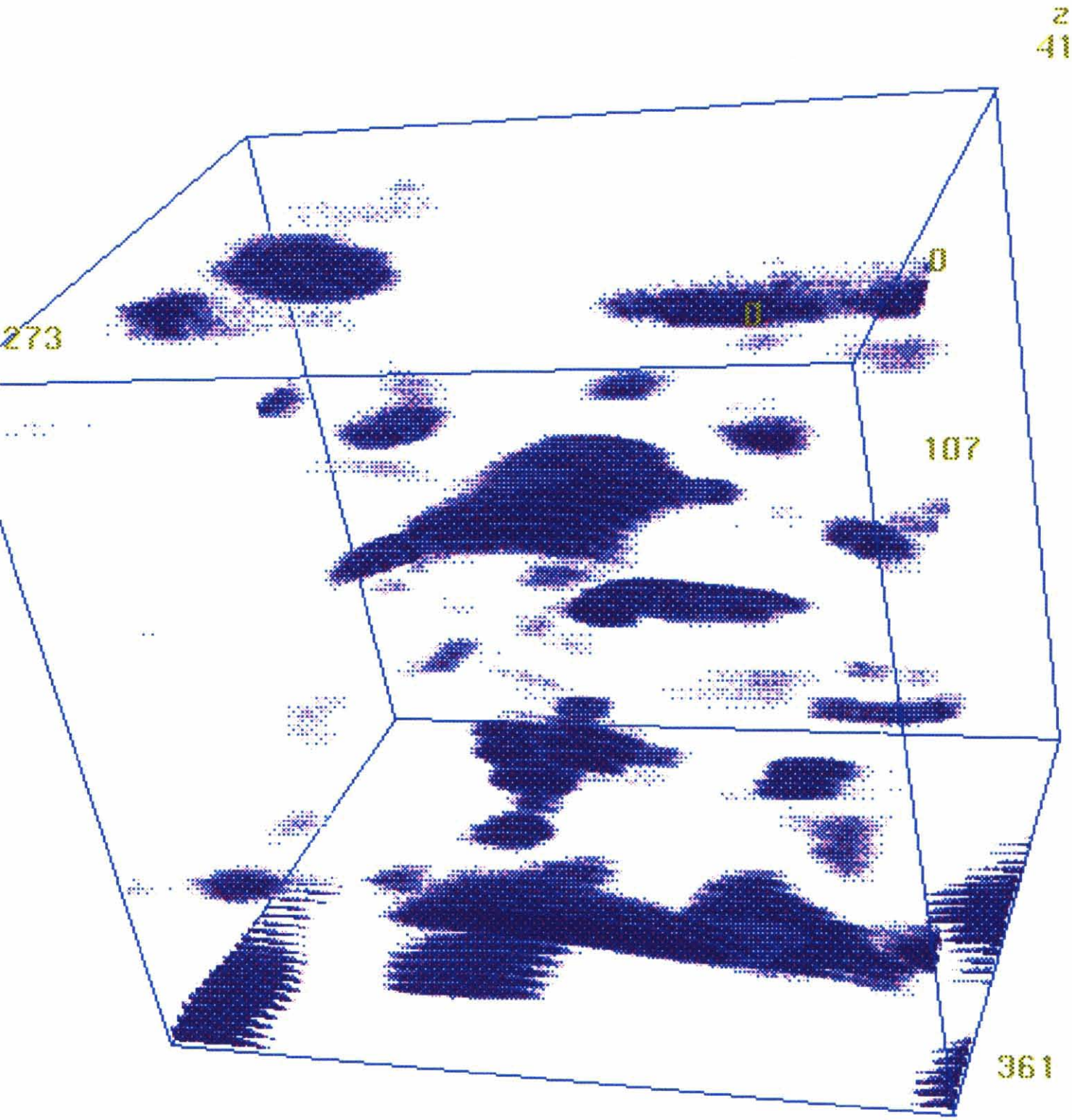


Medium conductor buried at 2 feet
Antennasparallel to traverse

## References

Daniels, J.J., 1994, Ground Penetrating Radar for Engineering Applications, ASCE Special Volume on Geophysical Methods ASCE Publication ISSMFE#10, XIII ICSMFE, New Dehli, 1994.

Daniels, J.J., Grumman, D., and Vendl, M., 1997, Vertical Incident Three Dimensional GPR: Jour. Env. Eng. Geoph., V.2, No.2, p1-9.

Roberts, R.L., 1994, Analysis and Theoretical Modeling of GPR Polarization Data: Ph.D. Dissertation, The Ohio State University, Columbus, Oh.